PROCESSING OF Fe Al BASED INTERMETALLIC THROUGH P/M ROUTE

by
SHANTANU DE

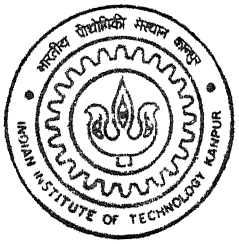

DEPARTMENT OF MATERIALS AND METALLURGICAL ENGINEERING
INDIAN INSTITUTE OF TECHNOLOGY, KANPUR

January, 2001

PROCESSING OF Fe Al BASED INTERMETALLIC THROUGH P/M ROUTE

A Thesis Submitted

in Partial Fulfilment of the Requirements

for the Degree of

MASTER OF TECHNOLOGY

by

SHANTANU DE

DEPARTMENT OF MATERIALS AND METALLURGICAL ENGINEERING

INDIAN INSTITUTE OF TECHNOLOGY, KANPUR

January, 2001

PROCESSING OF Fe Al BASED IMTERMETALLIC THROUGH P/M ROUTE

A Thesis Submitted

In Partial Fulfillment of the Requirements

For the Degree of

MASTER OF TECHNOLOGY

BY

SHANTANU DE

To The

DEPARTMENT OF MATERIALS AND METALLURGICAL ENGINEERING

INDIAN INSTITUTE OF TECHNOLOGY,KANPUR

JANUARY,2001

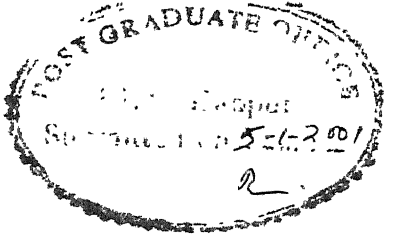

CERTIFICATE

This is to certify that the thesis entitled, PROCESSING OF Fe Al BASED IMTERMETALLIC THROUGH P/M ROUTE, is the record of the work carried out by SHANTANU DE under the supervision and has not been submitted else where for the award of a degree.

(Prof. S Bhargava)
Department of Materials and Metallurgical Engineering
Indian Institute of Technology
Kanpur

January,2001

ACKNOWLEDGEMENTS

I would like to express my deep sense of gratitude and indebtedness to Prof S. Bhargava for his valuable guidance, encouragement and inspirational discussion throughout the course of this investigation. It has truly been a learning experience to associate with him and work towards the completion of this work.

I am extremely thankful to Mr. M.k.Jadava for giving me valuable advice during the course of his thesis

I am grateful to Kumar ji, Umashankar ji, Mr.B.K Jain, Mr B.Sharma, Dr.M.N Mungolia and all staffs of MME dept. for their assistance in the experimental work.

I can not forget association and cooperation of my friend G.P.Dinda, Dulal, Projit for my thesis work.

January 5th 2001
I.I.T.Kanpur

(Shantanu De)

CONTENTS

LIST OF FIGURES

LIST OF TABLES

ABSTRACT

Iron-aluminium binary system consists of several aluminides, which are found to be attractive from the point of view of several engineering applications. These aluminides are, however, brittle in nature with essentially a nil cold-workability by conventional methods and therefore production of components from them requires novel processing routes to be developed. The present study is aimed to process single/multi-phase iron aluminide(s) by P/M route involving hot pressing. Thus a prealloyed iron aluminide powder comprising Fe_2Al_5-$FeAl_2$ phase mixture was mixed with pure iron powder ranging from 20 to 50 wt% and was hot pressed in uniaxial single acting hot press under the holding pressure ~ 25 MPa at the temperatures of 800°C, 850°C, 900°C and 950°C. The iron addition was found to improve the compressibility of the iron aluminide powder and also resulted in better densification. Fully dense microstructure of single/multi-phase iron aluminide compacts was obtained at hot pressing temperature 900 to 950°C. While two-phase $FeAl_2$-FeAl iron aluminide structures were obtained, with 20 and 30 wt % of Fe in the starting powder mixtures, a single phase FeAl structure formed in the case 40 and 50 wt % Fe additions. Relative density of the hot pressed products was found to increase with increase in hot pressing temperature Low hot pressing temperatures, i e 800 and 850°C, resulted in partially densified structures. Compressive strength of the material was found to increase with increase in hot pressing temperature.

It was also found that by keeping hot pressing temperature same if Fe% in the initial powder mixture is increased compressive strength value also increases.

CHAPTER ONE

INTRODUCTION

Intermetallic compounds are hybrid between superalloys and ceramics. These compounds have strength levels comparable to supperalloys with similar sensitivity to processing and operating conditions. On other hand ceramics are also stoichometric compounds with limited composition ranges, high melting temperature, and brittle behavior. A recent surge of research on intermetallics has taken place as ceramics failed live up to their promise and supperalloys has apparently been exhausted

Among the intermetallic compounds aluminide intermetallics are of much interest for future high temperature applications. This is primarily due to the benefits gained from their much lower densities and ability to withstand high temperature and corrosive environments as compared to existing alloys. Iron-aluminium binary system entails five stable intermetallic phases and three two phase regions in different composition ranges. Much of the work done on iron aluminides has been focussed on only FeAl (B2) and Fe_3Al (DO_3) single phase materials and order disorder transformation in this region. Inspection of the literature reveals that limited studies have been conducted on the Al-rich side of the Fe-Al system. It has been established that as %Al in iron aluminides increases, their brittleness increases and hence it is difficult to process Al-rich

phases of iron aluminide alloys by the conventional ingot metallurgy (I/M) routes. In contrast, routes based on powder processing offer the possibility of synthesizing such intermetallic alloys. Also if powder based routes have to be adopted they can also be utilised for the preparation of various multiphase aluminide based composites.

It is worth mentioning that such multiphase iron aluminides have been synthesized from elemental Fe and Al powders by the reactive sintering (RS) /reactive hot pressing (RHP) routes In contrast, the present study for synthesizing multiphase and single phase iron aluminide, involves pre-alloyed iron aluminide and iron powders. Iron was chosen for to serve two purposes, to increase the deformability of the powder mixture and to produce low Al content intermetallics.

Chapter two of the thesis briefly summarizes the literature on iron-aluminides, their properties & processing routes and ends with aims of present study. Details of the experimental procedure adopted have been presented in chapter three. Results obtained from the present study are discussed in chapter four Conclusions from present study have been summarized in chapter five.

CHAPTER TWO

LITERATURE REVIEW

2.1 INTERMETALLICS

Materials having high strength with the promise of sustainability at high temperatures have always been the prime focus of research in 20th century. This search for high temperature structural materials has stimulated much interest in the ordered intermetallics. Ordered intermetallics constitute an unique class of metallic materials that form long-range-ordered crystal structure (Figure 2.1) below a critical temperature that is generally referred to as the critical ordering temperature (T_c)[1-9]. These compounds are phases, which occur in the central part of the phase diagram between two or more metals with a characteristic crystal structure, and may have a very specific composition or a range of composition[10]. Because of the strong attraction between the unlike atoms involved, there is strong preference in the selection of nearest neighbours which in turn can lead to an ordered structure, a high resistance to deformation i.e. movements of lattice defects, and high melting point[1,2]. The high melting point in combination with the difficulty of movements of lattice defects, leads to high strength and retention of strength at elevated temperatures[6-8]. However, these same features, lead to very low ductility and intermetallic compounds display extreme brittleness at ambient temperatures[11-13].

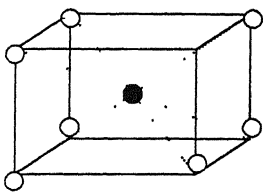

B2 or $L2_0$
(Fe, Co, Ni) Al

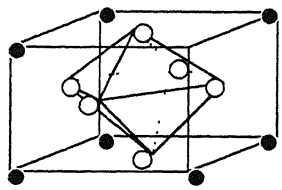

$L1_2$
Ni_3Al

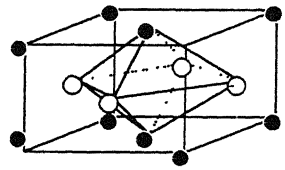

$L1_0$
TiAl

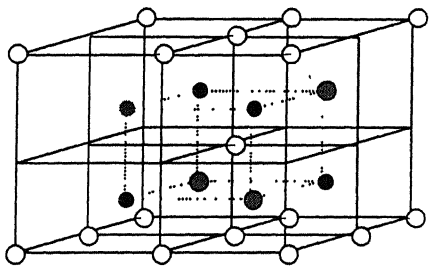

DO_3 or $L2_1$
Fe_3Al, Ni_2TiAl

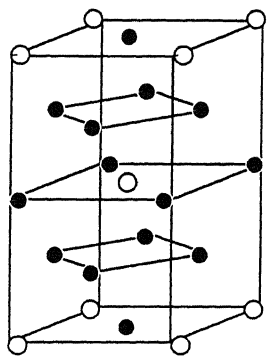

DO_{22}
$NbAl_3$

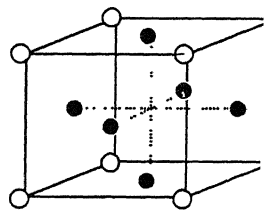

$L'1_2$
Fe_3AlC

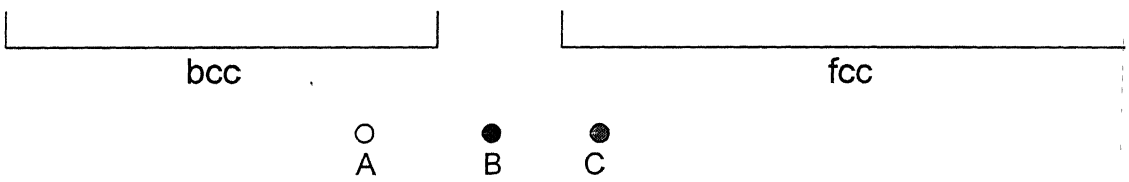

Figure 2.1: Crystal structures of some ordered intermetallic compounds

Various approaches have been used to overcome the problem of brittleness, while still retaining their high temperature properties. These approaches concentrate on (a) the microstructural control by altering the composition/processing and/or (b) incorporation of a ductile phase in the intermetallic matrix structure so that the micro-cracks get deflected during their propagation and thus increase the toughness.

Ordered Intermetallic alloys can be divided into several groups, e g Aluminides (e.g Iron, Nickel, Titanium), Trialuminides (e.g. $TiAl_3$, $ZrAl_3$, $FeAl_3$ etc.), Berylides ($NbBe_{12}$), Chromides (Cr_2Ti) etc. Some applications of intermetallics are shown in Table 2.1[2].

2.2 ALUMINIDES

Aluminides of iron, nickel and titanium, among various intermetallic compounds, have been the focuses of much of the research in the recent past. These aluminides possess many attributes that make them attractive for high temperature applications [Table 2 2][2]. They contain enough aluminium to form, in oxidizing environments, thin film of aluminium oxide (Al_2O_3), that often are compact and protective[14,15]. Aluminides have low density (due to presence of lighter aluminium in sufficiently high proportion), relatively high melting points, and good high temperature strength properties [Table 2.3]. But like other ordered intermetallics, they also exhibit brittle fracture and low ductility at room temperatures. Poor fracture resistance and limited fabricability restrict the use of aluminides as engineering materials[1,3-5].

Table 2.1: Some applications of intermetallic phases.

Phase	Application	Since about
Ni_3Fe	high permeability magnetic Alloy (Permalloy)	1920
FeCo(-2V)	soft magnetic alloy (Permendure)	1930
$Fe_3(Si,Al)$	magnetic head material (Sendust)	1935
$SmCo_5$	permanent magnets	1970
Nb_3Sn	A 15-superconductor	1965
CuZnAl, CuNiAl	shape memory alloys	1960
NiTi	shape memory alloys (Nitinol)	1965
$MoSi_2$	heater elements (Mosilit,Super-Kanthal)	1955
NiAl, CoAl	protective coatings	1965

Table 2.2 : Applications of Structural Intermetallics

Ni_3Al	- Diesel - engine turbocharger rotors; - High - temperature dies and molds; - Air craft parts; - Turbine blades, - Hydro turbines;
Fe_3Al	- Toasters, stoves, Ovens, - Automotive gas turbines engines; - Coal - gassification system; - Insulating wrappings for investment casting; - Components needing high temperature sulfidation resistance;
Ti_3Al	- Transition duct support; - Seal housing; - Compressor starters; - Turbine frames; - LP turbine airfoils.

Table 2.3: Important Aluminides and Their Relevant Properties

Alloy	Crystal Structure	Melting Point(^{0}C)	Density (g/cc)	Yield Strength (MPa)	Young's Modulus (X10^{3}Mpa)
Ni_3Al	$L1_2$ (Ordered fcc)	1190	7.5	250-300	178.6
NiAl	B2 (Ordered bcc)	1640	5.9	250-475	294.4
Fe_3Al	DO_3(Ordered bcc)	1540	6.7	385-392	140.7
FeAl	B2 (Ordered bcc)	1250	5.6	360-380	260.6
Ti_3Al	DO_{19}(Ordered hcp)	1600	4.2	700-990	144.8
TiAl	$L1_0$(Ord. Tetragonal)	1460	3.9	400-650	175.8

In recent years, alloying and processing have been employed to control the ordered crystal structure, microstructural features, grain boundary structures and composition to overcome the brittleness problem in ordered intermetallics.

2.3 IRON ALUMINIDES

The most studied iron aluminides are FeAl and Fe_3Al. The combination of low density, excellent oxidation and sulphidation resistance, and lack of strategic alloying elements make these alloys particularly attractive. However the major drawbacks of iron aluminides are their low ductility and fracture toughness at ambient temperatures and their poor strength at elevated temperatures i.e. above 600^0C[14,15]. Recently, considerable efforts have been devoted in improving their mechanical properties through control of grain structure, alloy addition and material processing.

2.3.1 Iron – Aluminium Binary System

2.3.1.1 Phase Diagram

Fe-Al binary phase diagram is shown in Figure 2.2[10] Fe-Al system is characterised by a wide α-Fe solid solution range. The ordered α_2(FeAl) region is divided into different fields. The system entails five stable phases, namely Fe_3Al, ε, $FeAl_2$, Fe_2Al_5, and $FeAl_3$, each of them with a homogeneity range. There are also two metastable phases Fe_2Al_9

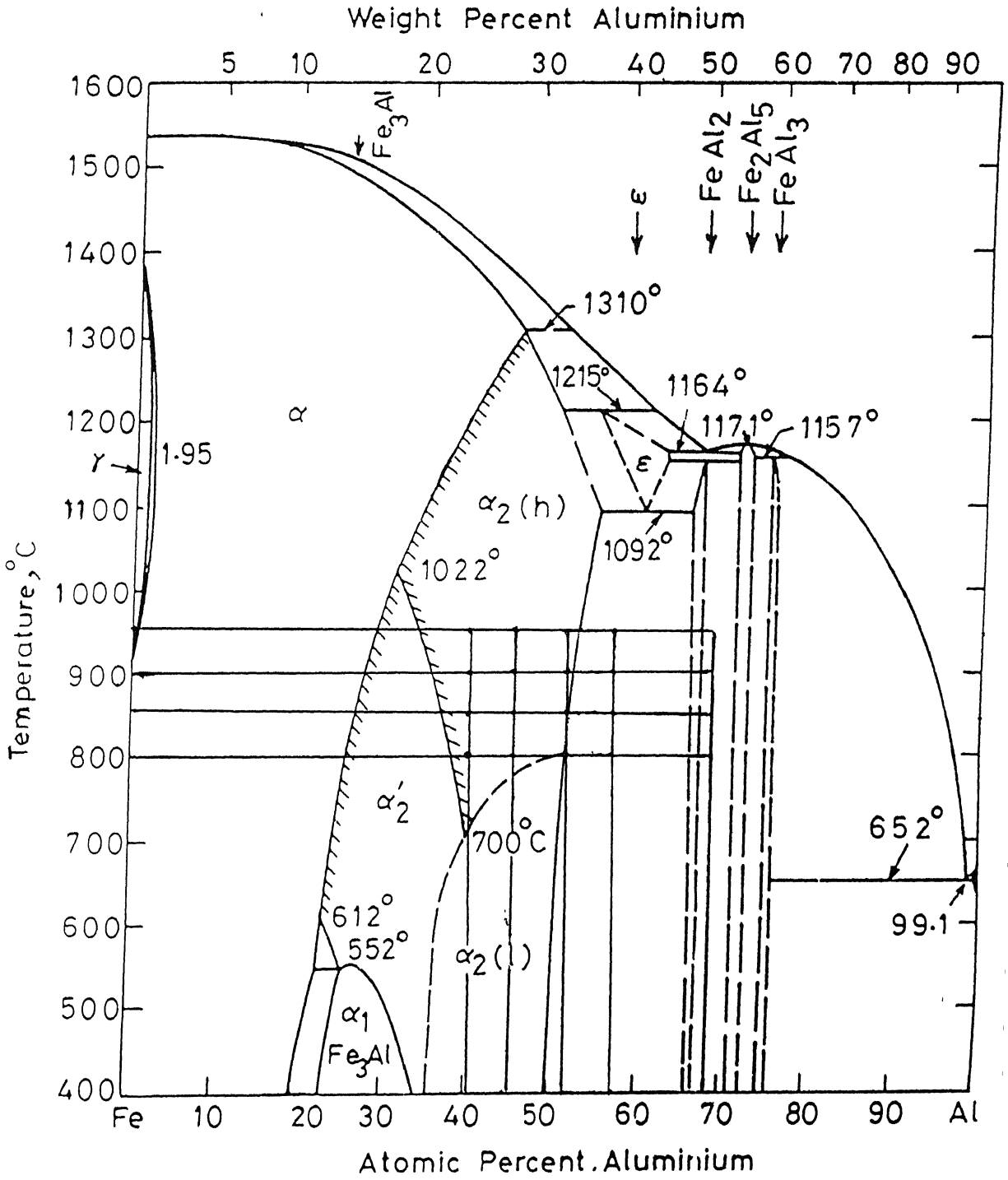

Figure 2.2 :Fe-Al Binary Phase Diagram

and $FeAl_6$ The addition of Al to Fe hardly changes the course of the liquidus/solidus between 0 and 10 at% Al. They then fall smoothly to 1310^0C, where a peritectic reaction occurs corresponding to:

$$L(50.7at.\%Al)+\alpha\text{-}Fe(45.2at.\%Al)=FeAl(\alpha_2).$$

In Figure 2.2 the formation of α_2(FeAl) is not shown as a peritectic reaction, but as a second order reaction concordant with the Fe-Si and Fe-Ga system. Values for the limits for the α- and γ- region is found to be 1.285 and 1.95 at% Al. However the α_2(B2) region, which is considered to be homogenous, is subdivided: α_2(FeAl) occurring reversibly in high and low temperature modification. The transformation takes place at 830^0C and is composition dependent. On the other hand, α_2(high) transforms into α_2' which is demonstrated by thermal analysis and a change in volume; and α_2' again changes into the ordered structure DO_3 (Fe_3Al) by a first order reaction. The transformation of the latter takes place at 552^0C and 26 8 at % Al. The phase boundaries of ε are still some what uncertain It is high temperature phase, formed by peritectic reaction at 1215^0C as follow.

$$\varepsilon\ (54.33\ at.\%Al) = \alpha_2(49.9at.\%Al) + L(60.18at.\%Al).$$

$FeAl_2$ is formed by a peritectoidal reaction at about 1153^0C. There is general agreement about the congruent formation of Fe_2Al_5. The melting point of stoichiometric Fe_2Al_5 is 1171^0C The Al-richest phase $FeAl_3$ is formed peritectically at 1157^0C.The maximum solid solubility of Fe in Al is about 0.03 at.% at 625^0C.

2.3.1.2 Crystal Structure:

The stable phases studied very much are Fe_3Al and FeAl, which have DO_3 and B2 ordered superlattice structure respectively. Both of these crystal structures are derivatives of BCC structures existing at room temperature over a range of 18 at% to nearly 36 at% Al respectively. The ordered DO_3 structure consists of eight BCC cells with each unit cell consisting of sixteen atoms. B2 structure on the other hand, has two interpenetrating simple cubic lattices with the atoms of each constituent at the body center of each other (Figure 2.3).

The ϵ phase was suggested to be complex bcc with 16 atoms per unit cell and the ς phase ($FeAl_2$) to be rhombohedral with 18 atoms per unit cell. The structure of the latter phase was claimed to be more complicated[26].

The η phase (Fe_2Al_5), first believed to be monoclinic with 56 atoms per unit cell, was reported to be orthorhombic, with 'a=7.67 A, b=6.40 A, c=4.20A' for 72 0 at% Al.

The θ phase ($FeAl_3$) was previously believed to be orthorhombic. A complete structure analysis, using specimen with about 76.5% Al, revealed the structure to be monoclinic with 100 atoms per unit cell and a=15.489 A, b=8.083 A, c=12.476 A, $\beta=107^{o}43' \pm 1'$[26].

The existence of unstable Fe_2Al, claimed to be present in a complex Fe-Ni-Cr alloy, was reported by Beattie et al [25]. It was stated to be isotopic with $MgZn_2$.

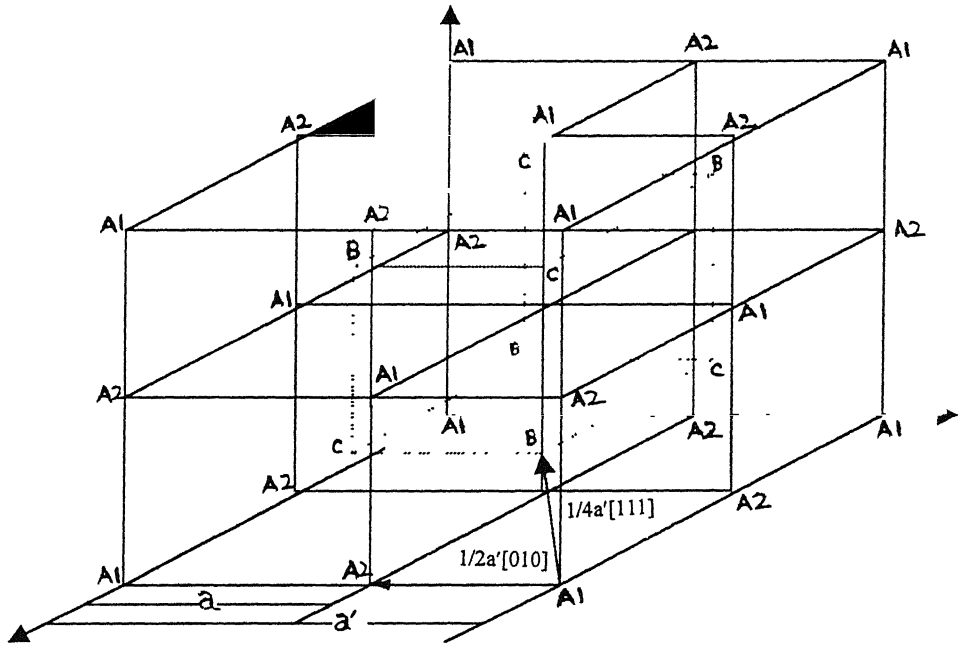

(a)

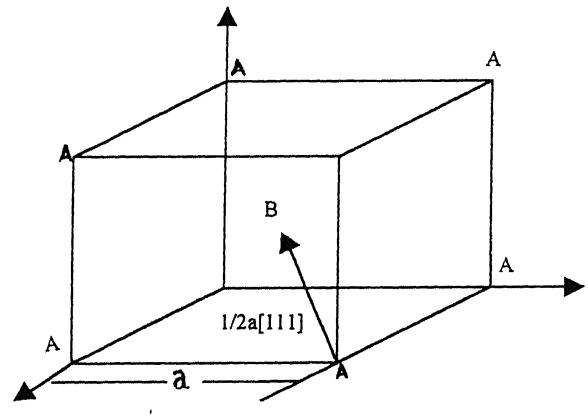

(b)

Figure2.3: The unit cell and APB for the (a) DO_3 and (b) B2 superlattices. A, A1, A2, C Fe sites. B represents Al sites.

A phase characterized as $FeAl_6$ is C-centered orthorhombic isotopic with $MnAl_6$ with a=6.492A, b=7.437A, c=8.788A. Investigations state that this phase is metastable at ≥538°C ; there is no evidence of it being an equilibrium phase[27]. Other information regarding crystal structures of iron aluminides are presented in table 2.4[6] and 2.5[7].

2.3.2 Defects in Ordered Fe-Al Intermetallics:

The unit cell for the DO_3 and B2 lattices characteristic of Fe_3Al and FeAl are shown in Figs 2.3(a) and 2.3(b). In these each Al atom has only Fe nearest neighbors but the second nearest neighbors are Fe in DO_3 structure and Fe and Al at random in B2 structure. Anti-structural vacancies appear to form on Fe sites in FeAl at Al contents >50%[8]. Vacancies may be formed in the iron aluminides by quenching from high temperature. Field ion microscopy showed that Fe-49.5% Al quenched from 1273 K contained a high (1.85 ± .05at%) concentration of quenched-in vacancies , with their concentration being approximately twice as high on Fe sites as on Al sites.

For stoichiometric composition, maximum order means that there are no vacancies present and Fe and Al atoms occupying their own sites. For off-stoichiometric compositions, maximum order means that no vacancies exit and the excess Fe atoms substitute to other atom sites. For Fe-Al alloy the frequently occurring defect is the triple-defect, consisting of a Fe atom on the Al-site, and two vacancies on the Fe-site; the Al atoms do not appear to substitute for Fe atoms[30].

Table 2.4: Crystal Structure Data of Fe-Al intermetallics

Phase	% wt Al	Pearson Symbol	Space Group
α-Fe	0 - ~28	CL2	Im$\bar{3}$m
γ-Fe	0 - ~0 6	cF4	Fm$\bar{3}$m
FeAl	12.8 - ~37	cP8	Pm$\bar{3}$m
Fe_3Al	~13 - ~20	cF16	Fm$\bar{3}$m
∈	40 - ~47	cL16	--
$FeAl_2$	48 - ~49.4	aP18	P1
Fe_2Al_5	53 – 57	oC	Cmcm
$FeAl_3$	58.3 – 61.3	mC102	C2/m
Metastable			
Fe_2Al_9	68.5	mP22	$P2_1/c$
$FeAl_6$	74.3	oC28	$Cmc2_1$

Table 2.5 Lattice parameters of iron aluminides

Phase	a-b-c (nm)	α-β-γ(^{o})	Structure type
FeAl	0.2909	90 90 90	BCC
Fe_3Al	0.57923	90 90 90	BCC
$FeAl_2$	0.4878 0.6461 0 8800	91.75 73.29 96.89	Complex
$FeAl_3$	1.5489 0.8083 1.2476	90 90 107.72	Monoclinic
Fe_2Al_5	0.7675 0.6403 0.4203	90 90 90	Orthorhombic

In B2 FeAl (Figure 2.3), dislocation configuration consists of two like a/2<111> dislocations connected by the corresponding a/2<111> antiphase boundary (APB), 'a' being lattice parameter of the B2 unit cell.

The DO_3 dislocation configuration consists of four like a'/2<111> dislocations connected by two types of APBs: (1) the outer pairs of dislocation are connected by an a/2<111> (a'/4<111>) APB which is affected mainly by first nearest neighbour interaction energies and is similar to a B2 APB , and (2) the inner pair of dislocation are connected by an a'/2<100> APB which is affected by second nearest neighbour interaction energies . Here 'a' is the lattice parameter of DO_3 unit cell.

Formation of the DO_3 structure may be suppressed by quenching alloys from temperatures above DO_3 ordering temperature (T_C). In such cases, the alloys have an imperfect B2 structure and may exhibit B2 dislocation configuration.

2.3.3 Properties of Ordered Fe-Al alloys

2.3.3.1 Crystallography of Slip & Twinning

Slip systems in B2 Fe-Al alloys at 298 K have been reported to be {110} <111>[12]. Slip in FeAl single crystal is a strong function of orientation and deformation temperature. At about 0.44 T_m there is a gradual transition from <111> to <001> slip with increasing temperature. The dislocation arrangement in crystals deformed by <001> type slip consists mostly of edge dislocations There is also a composition dependence of the slip mode. The slip system in DO_3 alloys is {110}<111>. Cohn and Coll[9] have shown that in a DO_3 Fe-23.5% Al alloy, mechanical twinning occurred when the degree of long range order

was 0.5 or less. Twinning is more easily accomplished in the B2 than in the DO_3 modification of Fe_3Al

2.3.3.2 Strength

The hardness (H)[12] of B2 Fe-Al alloys varies with temperature according to the relation $H = Ae^{-BT}$, where A and B have one set of values at low temperatures and another set at high temperatures. At low temperatures, the hardness increases with increasing Al content, while at temperatures greater than 873 K, this behaviour is reversed.

The effect of aluminium content on the yield strength and ductility in 24 at% to 30 at% Al was studied by Mckamay et al[7] (Figure 2 4). There is a gradual drop in yield strength (from 800 to 300 MPa) accompanied by a steady increase in ductility (from 1 to 5 % tensile elongation) with increasing Al content in DO_3 Fe-Al alloys. Also, the transition from high stress value at 26 at% Al to a lower value at 27 at% Al coincides with the boundary between the α+DO3 and DO_3 phase fields at 800°C in the Fe-Al phase diagram (Figure 2.2). Based on this, Inoye[7] has shown that the higher ambient strengths at 24-25 at % Al composition is due to age hardening effect of α-precipitated in DO_3 phase during the ordering treatment at 800°C in these compositions. The ductility increase from 1% at 24 at% Al to 5% at 30 at% Al is apparently associated with the drop in yield strength resulting from increasing Al content.

Alloying studies to raise the transition temperature have been successful in improving the strength levels up to 800°C[12]. Figure 2.5

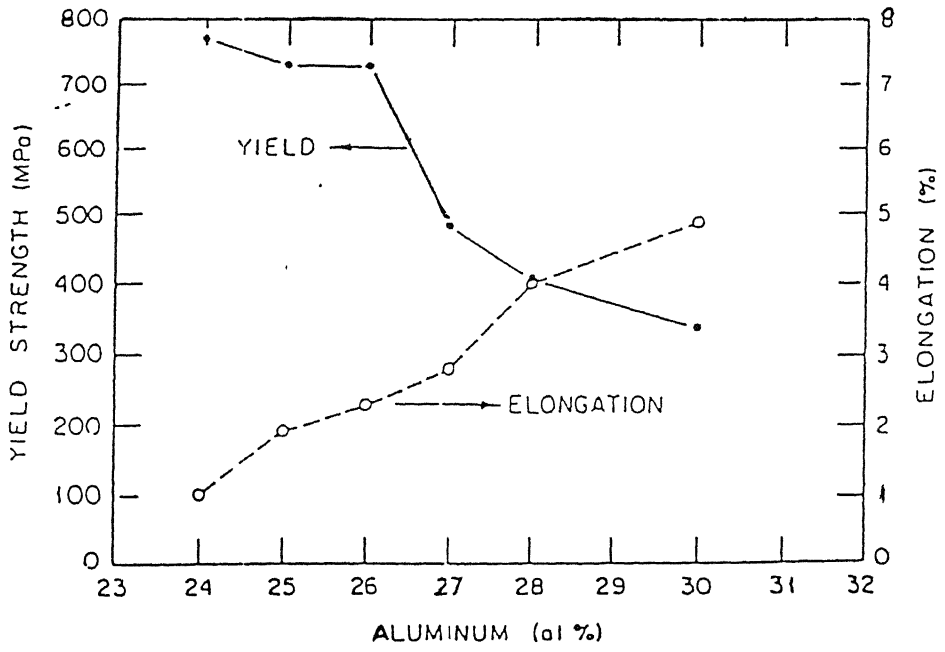

Figure 2.4 Plot showing variation of Yield strength and ductility with Al content

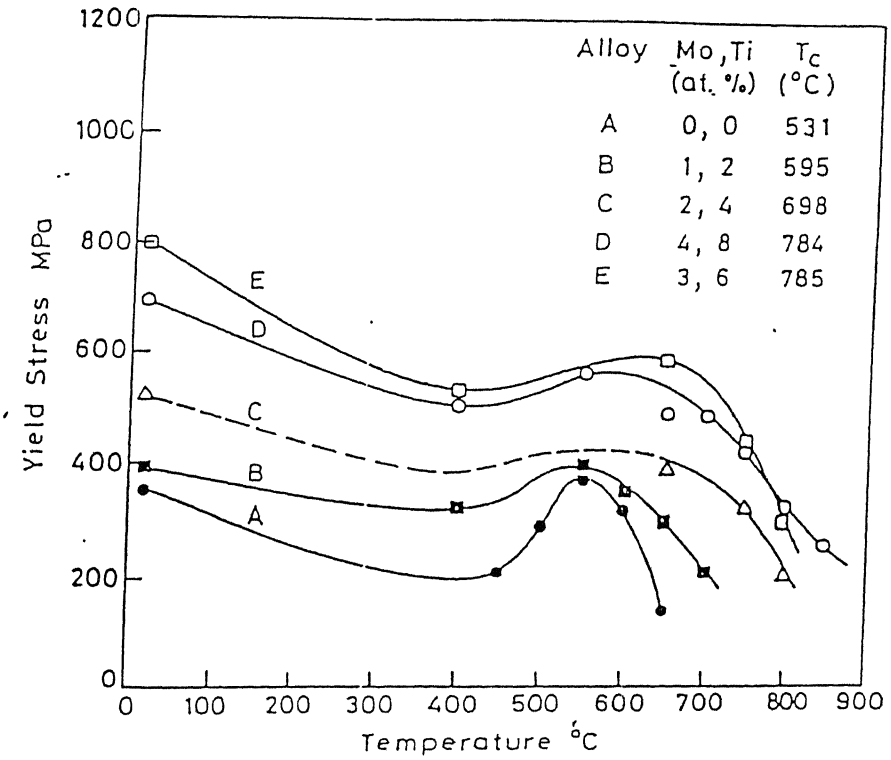

Figure 2.5: Yield Strength vs Temp plot for alloyed Fe_3Al

shows a typical compressive yield stress plot with temperature of Fe_3Al alloyed with different amounts of Mo & Ti with their respective transition temperatures. The strength peaks in Fe_3Al alloy may be explained by considering the dislocation structure in these alloys. The increase in room temperature hardness and yield strength with increasing Al-content has since been observed by several investigations B2 Fe-Al (32 to 50%) alloy may show significant strengthening arising from retention of non-equilibrium vacancies even during conventional air-cooling.

2.3.3.3 Work Hardening

The work hardening behavior actually observed to be dependent on the deformation temperature (which affects the nucleation of dislocation as the degree of DO_3 order increases in Fe_3Al alloy, work hardening also increases), the degree of order of the material and its composition which determine the APB energies and hence the shear stresses required to produce them

2.3.3.4 Ductility

As shown in Figure 2 4, there is an increase in ductility with increasing Al content in DO_3 Fe-Al (24 at% to 30 at% Al) alloys. Room temperature ductility of polycrystalline Fe-Al alloys decreases rapidly with the onset of ordering. For Fe-Al alloys containing more than 30 at% Al, the ductility shows a general trend of decreasing with increasing Al level at temperatures up to 400°C. At higher temperatures, the alloys exhibit a peak ductility around 35-38 % Al. FeAl is brittle at higher Al contents because it fractures at grain boundaries before yielding. Lower Al content

reduces the yield stress substantially and hence some ductility is observed before fracture.

A number of workers have reported on the elevated temperature ductility of ordered Fe-Al alloys. 100 % elongation were obtained in creep tests on DO_3 Fe-27.8 % Al alloys at 826 K. Elongation of 12-16 % were reported for B2 Fe-Al alloys containing 39-40 % Al in compression tests conducted at 1300K[19].

2.3.3.5 Fracture

As stated earlier, iron aluminides are inherently brittle at room temperature. The iron aluminides show low tensile elongation at room temperature and fracture mainly by cleavage for alloys with less than 40 at% Al and by brittle grain-boundary separation for alloys with more than 40 at% Al[12] Proposed modes of fracture of Fe-Al alloys are summarized in Table 2.6[12].

The major cause of low ductility and brittle fracture of iron aluminides is mainly by an extrinsic effect i e. environmental embrittlement. The yield strength is insensitive to environment, and the ultimate tensile strength correlates with the tensile elongation, which depends strongly on test environment. The iron-aluminides (Fe-36.5 at% Al) had ductility of 2% in air, 6% in vacuum and 17.6% in dry oxygen. The lowest ductility was observed in samples tested in water vapour and the samples tested in molecular hydrogen did not cause severe embrittlement of iron-aluminide, so this test indicates that moisture in air is the embrittling agent.

Table 2.6 : Modes of Fracture in Ordered Fe-Al Alloys

1	Cleavage on {100} Planes by <100> edge dislocations.
2	Cleavage failure due to hydrogen embrittlement.
3	(a) Cleavage failure due to dislocation APB interactions.
	(b) Intergranular failure in absence of these interaction.
4.	Intergranular failure due to dendritic structure.
5.	Failure at grain boundaries before yielding in bulk.
6	Intergranular failure due to weak grain boundaries.

Environmental embrittlement has been explained by the following reaction :

$$2Al + 3H_2O \rightarrow Al_2O_3 + 6H^+ + 6e^-$$

The reaction of moisture in air with aluminium atoms at crack tips results in the generation of high fugacity atomic hydrogen that rapidly penetrates into the crack tips and causes severe embrittlement. The highest ductility is generally obtained in a dry oxygen environment, (rather than in vacuum) because oxygen reacts with the aluminium to form aluminium oxide directly, thereby suppressing the aluminium-moisture reaction and the generation of atomic hydrogen. It should be noted that the maximum degree of moisture induced hydrogen embrittlement occurs around ambient temperatures. At higher temperatures, less hydrogen is concentrated at crack tips, and in-situ protective oxide films can form more readily on specimen surfaces; whereas at lower temperatures, the aluminium-moisture reaction is slowed, and the equilibrium moisture content in air is lowered.

The environmental sensitivity of FeAl is markedly reduced when the aluminium concentration is higher than 38 at%. For Fe-43 at% Al, the ductility is almost nil in air as well as in dry oxygen; all specimens fail intergranularly. The lack of an environmental effect is explained by the fact that the grain boundaries in FeAl alloys with Al>38 at% are intrinsically brittle. Therefore, environmental embittlement and intrinsic grain-boundary brittleness must both be recognized in order to establish strategies for reducing overall brittleness in FeAl alloys. This, intrinsic grain boundary brittleness in FeAl as well as other intermetallics, can be

alleviated by microalloying with boron, which tends to segregate to the boundaries and enhance their cohesive strength.

Similar air embrittlement has been observed in Fe_3Al alloys. The moisture-induced hydrogen affects not only tensile properties, but also the fatigue and crack growth behavior. Under cyclic loading conditions, vacuum or oxygen environments raise the fatigue threshold and reduce crack growth rates at ambient temperatures. The degree of embrittlement under cyclic loading conditions is also affected by the crystal structure of Fe_3Al. The DO_3 structure in a Fe_3Al alloy shows a crack growth rate much faster than that in the B2 structure, indicating that the DO_3 structure is more susceptible to environmental embrittlement in air.

2.3.3.6 Creep and Fatigue

The creep resistance of ordered intermetallics may be expected to be better than that of disordered alloys because of slower diffusion in the ordered lattice as well as because of more difficult glide processes[12]. The creep resistance of the binary Fe_3Al alloy is relatively mediocre, but additions of small quantities of Mo and particularly Nb lead to considerable improvements in creep rate and life[18]. These improvements have been attributed to improved solution hardening (for Mo) which reduces the rate of dislocation recovery, as well as to (for Nb) particle dispersion strengthening.

For B2 Fe-Al alloys of Al content 41 to 49 at%, Whittenbergher[19] investigated creep phenomena in the temperature range 1100 to 1400 K and established that :

(a) The activation energy for creep in these alloys was independent of composition.

(b) Deformation may occur by two different and apparently concentration independent mechanism. One with a stress exponent of about 6 and the other with an exponent of about 3.

(c) Both the deformation mechanisms are dependent on grain size but in opposite manner. For the low stress exponent mechanism the strength increased with increasing grain size and vice-versa.

(d) Under the high stress exponent mechanism a large-angle grain boundary structure may be replaced by a small-angle structure of similar grain diameter.

The study of high cycle fatigue behavior of DO_3 and B2 polycrystalline Fe_3Al (Fe-23.7 at% Al and Fe-28.7 at% Al), reveals that DO_3 order is effective in prolonging fatigue life only in Fe-28.7 at% Al at 298K. This can be explained by the presence of superlattice dislocations, which are not observed in Fe-23.7 at% Al. This has been attributed to restrictions on cross slip imposed on superlattice dislocations, which delay crack initiation. The fatigue properties of B2 alloys found to degrade sharply with increase in temperature. Among DO_3 alloys, Fe-23.7 at% Al shows little loss in fatigue life with increase in temperature

which is attributable to its two phase microstructure while Fe-28.7 at% Al shows a sharp drop with increase in temperature over a range of 293 to 773 K[16]. At temperatures above the two-phase field, the fatigue life falls sharply as a result of creep-fatigue interaction. Here, crack initiation occurs at grain boundary near specimen surfaces, but propagation is predominantly by transgranular cleavage.

2.3.3.7 Corrosion Resistance

The iron aluminides are highly resistant to oxidation and sulfidation at elevated temperature. As stated earlier, resistance stems from the ability of the aluminides to form highly protective Al_2O_3 scales. The oxidation resistance generally increases with increasing Al content, the major products are α-Al_2O_3 and trace amounts of iron oxides when the aluminides are oxidized at temperatures above 900°C. Cyclic oxidation of Fe-40 at% Al alloyed with upto 1 at% Hf, Zr and B, produced little degradation at temperatures up to 1000°C. Aluminides specimen tested at 700 to 870°C showed no indication of attack in sulfidising environments, except for the formation of a thin layer of oxides with a thickness in an interface colour change. Further, iron aluminides exhibit corrosion rates lower than those of the best existing iron-based alloys by a couple of orders of magnitude when tested in a severe sulfidising environment at 800°C. In addition, the aluminides with more than 30 at% Al are very resistant to corrosion in molten nitrate salt environments at 650°C.

2.4 PROCESSING ROUTES FOR IRON ALUMINIDES

Various processing routes followed for production of intermetallic parts are shown in Figure 2.6 as a flow chart. These routes are discussed in detail in following subsections.

2.4.1 Ingot Metallurgy Route

Ingot metallurgy route[24] has been the focus of attention for the production of Ti_3Al, Ni_3Al, Fe_3Al based aluminides for a long period, despite the fact that this route has many problems. The primary fabrication process using the traditional methods of melting and casting poses serious problems, like the alloy inhomogeneity, the elemental losses, the casting defects, fracturing defects etc. The secondary fabrication to obtain necessary shapes and sizes by further deformation and machining, poses still further problem as the aluminides are generally brittle in nature.

2.4.1.1 Melting

Air melting is feasible for iron aluminide alloys. Reasonable, but not exceptional, care is needed in treating the melt charge and the selection of crucible material. Both the iron and aluminium need to be dried to minimize the generation of hydrogen. Because of the reaction of aluminium with moisture, a large amount of hydrogen can be generated and dissolved in liquid metal. It is the rejection of this hydrogen during solidification that causes the gas porosity in iron aluminides. Typical

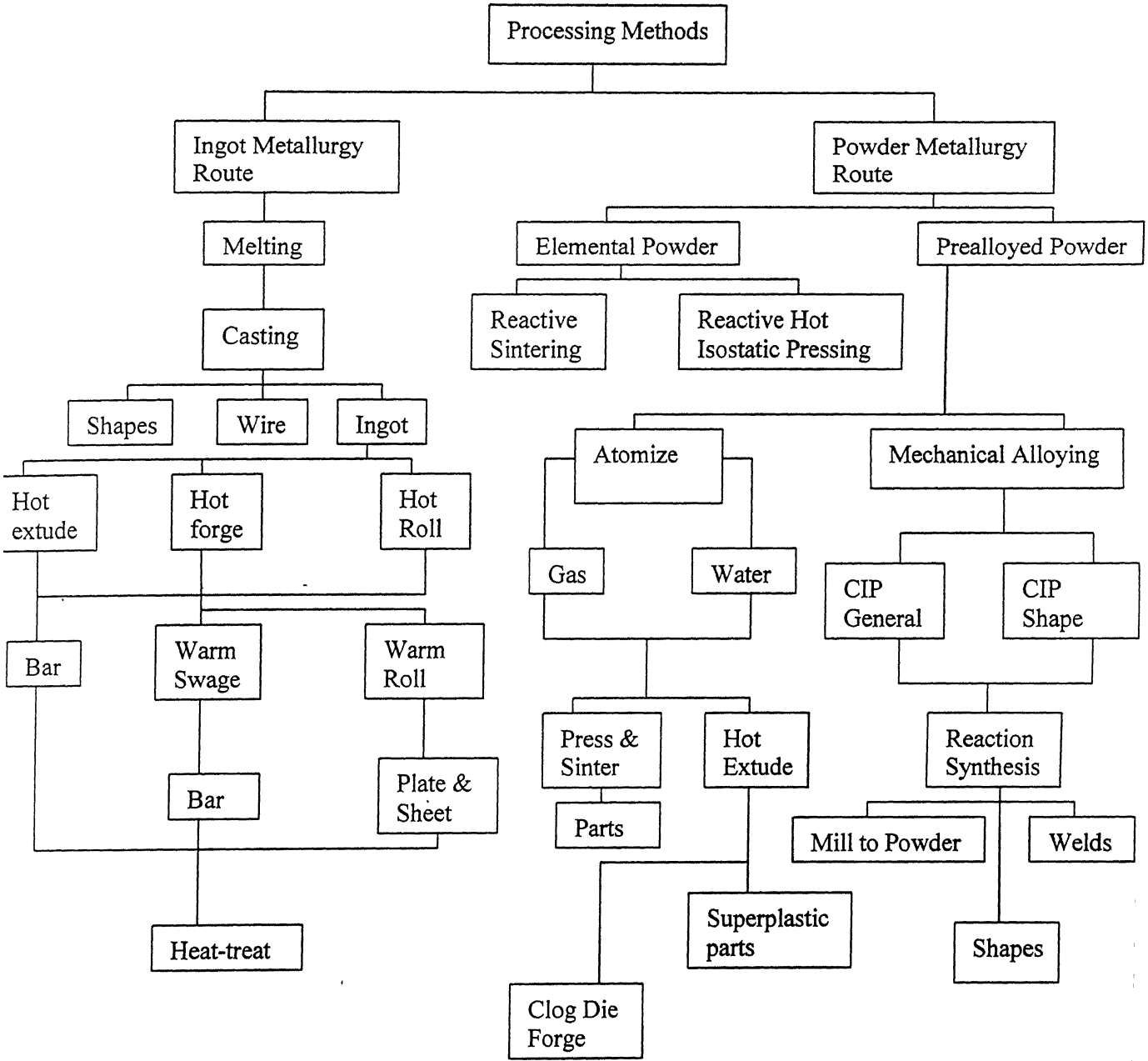

Figure 2.6 Processing routes used to produce intermetallic parts.

hydrogen levels in the Fe_3Al alloy melted in air can be in the range of 3 to 4 ppm. The hydrogen level of the alloy can be further reduced to approximately 2 ppm by blowing argon through the melt. Vacuum melting of the alloy can yield hydrogen level as low as 1 ppm. The protective alumina oxide slag formation during melting yields low levels of oxygen and nitrogen in the melt and also provides nearly 100% recovery of most of the alloying elements. A combination of vacuum melting and electro-slag remelting processes further reduce oxygen and nitrogen contents of the Fe_3Al based alloys.

2.4.1.2 Casting

The Fe_3Al based alloys are castable in to shapes by both sand and investment casting processes. The casting parameters such as type of sand, melt superheat, cooling rates and post-cast treatments are not fully developed for sand castings. In case of investment castings, issues such as shell material, use of grain refiner, shell temperature, melt superheat, cooling rates, and post cast treatments need additional work The low room temperature ductility in the as cast condition is the primary concern in the handling and use of castings.

2.4.1.3 Mechanical Working

Fe_3Al based alloys are hot workable with typical hot working temperature ranging between 900 –1100°C. The hot worked material can be warm finished at temperature as low as 180°C. The Fe_3Al based alloys are not cold workable.

2.4.2 Powder Metallurgy Route

Powder metallurgy processing is becoming increasingly important for obtaining desirable microstructures, improved properties, and near net shape manufacturing capabilities for iron aluminides. Also, powder metallurgy processes bypass requirement of melting and casting large ingots and thus greatly reduce the problems associated with them. There are two types of powder metallurgical processes, one uses prealloyed aluminide powder and second uses elemental Fe and Al powders as starting materials.

2.4.2.1 Powder Metallurgical Processes Based on Elemental Fe and Al Powders.

Reactive sintering (also known as combustion synthesis, or self – propagating high temperature synthesis) is a novel process to produce ordered intermetallics from elemental powders through self-sustaining reaction. This approach utilizes an exothermic reaction between powder constituents to synthesize compounds[28]. Process advantages include the use of inexpensive and easily compacted elemental powders, low processing temperatures, short processing times and considerable flexibility in terms of compositional and microstructural control. Depending upon thermodynamic properties and phase diagram features, a variety of reaction products are possible, ranging from highly porous to full dense materials.

Reactive sintering is controlled by a transient liquid phase that forms during rapid exothermic heating. The initial compact is composed

of mixed powders, which are heated to a temperature where they react to form a compound product. Here, a stoichiometric mixture of A and B powders is used to form an intermediate compound product AB. The reaction occurs above the lowest eutectic temperature in the system yet at a temperature where the compound is solid. Heat is liberated because of the stability of the high melting temperature compound. Consequently, reactive sintering is nearly spontaneous once the liquid forms. The liquid provides a capillary force on the structure, which leads to densification. The liquid is transient as the process is conducted at a temperature below the melting point of the compound, typically near the eutectic. Reaction sintering involves a transient liquid phase, duration and amount of which depends on several processing parameters and which in turn controls the sintering characteristic. The reaction sintering is highly sensitive to parameters such as amount of additive and the particle size, green density of initial compact, heating rate, sintering atmosphere and sintering time

The intent of prior studies on Fe-Al was not to form intermetallic compounds as products, nevertheless, the observations reported emphasize the problems encountered in this system. Elemental iron-aluminium mixture represents a particular challenge for powder processing because of extensive swelling during sintering. Swelling is predicted based upon phase diagram features (Figure2.2), notably, there is a large solubility for aluminium in iron, low reverse solubility, and a large melting point difference, suggesting imbalance diffusion rates.

Systems that exhibit a large driving force for compound formation are particularly susceptible to the formation of porosity during alloying. Synthesis of iron aluminide from elemental powders has been reported in the literature. Reaction chemistry in Fe-Al, studied using differential scanning calorimetry (DSC) is shown in table 2.7.

The conventional reactive sintering involves no pressure i.e. it is pressureless sintering. The highest sintered densities obtained by Rabin and wright[28] were approximately 75% of the theoretical for Fe-15wt%Al and 69% of theoretical for Fe-32wt%Al in pressurless reactive sintering. The higher sintered density can be obtained by applying an external pressure to the compact during sintering. This process is known as hot pressing. Here, pressure assisted densification is carried out by applying a load to the samples during the exothermic reaction. Rabin and

Table 2.7: Reaction chemistry of Fe-Al

Atom%	reaction Temp.(K)	Heating-rate k/Min	$-H^0_{298}$ KJ/g atom	phase Present
50 Fe-50 Al	911	15	19.6	FeAl, Fe_2al_5, Fe
75 Fe-25 Al	916-984	15	7.89	Fe_3Al, Fe

Wright also observed the effect of applied pressure on density for both the compositions. Near full density was achieved for both compositions when an applied pressure of 70 MPa was used. Significantly higher densities were also obtained for a given applied pressure when the larger powder charge was used. This suggests that the larger thermal mass resulted in slower cooling from the reaction temperature, thus allowing more densification to take place.

2.4.2.2 Powder Metallurgical Processes Based on Prealloyed Iron-Aluminide Powder

Though iron aluminides can be prepared by reactive sintering of elemental powders of iron and aluminum, this method does not have such control and flexibility as synthesis from prealloyed iron aluminide powders

Mechanical alloying, rapid solidification and physical vapor deposition, far from equilibrium techniques for synthesis of prealloyed iron aluminide powders allow novel constitutional and microstructural effects and hence potentially enhanced physical and mechanical properties in powders and therefore in products made from them.

Mechanical alloying (MA), a solid state powder processing technique, has been employed to synthesize a variety of alloy phase starting from either blended elemental or prealloyed powder. The repeated welding, fracturing, and rewelding of powder particles can lead to the formation of supersaturated solidsolutions, crystaline and quasicrystalline intermediate phase, and metallic glasses. The grain size

of the crystalline phases produced by this technique is often of nanometer dimensions, and these nanocrystaline materials can exhibit an excellent combination of properties making them potentially attractive for a number of applications. Recently there have been many investigation on the synthesis of intermetallic compounds by MA. However, in majority of these cases the synthesis of the intermetallics only on heat treatment of MA powders, Only in a few cases is the formation of the intermetallics achieved directly by MA; some of these phases are in ordered state, although the ordering is far from complete.

These techniques lead to various combinations of the following attributes in powder:

1) Production of, a fine dispersion of second phase particles.
2) Extension of solubility limits
3) Refinement of the matrix microstructure down to the nanometer range.
4) Synthesis of novel crystalline phases.
5) Development of amorphous (glassy) phases.
6) The possibility of alloying elements which are difficult to alloy.
7) Inducement of chemical reaction at low temperatures.
8) Scalable process.

These attributes can be maintained in the product made out of these pre alloyed powders by proper processing.

Prealloyed intermetallic powders are generally brittle and therefore it is difficult to process them via classical P/M route. Hot

pressing, Hot isostatic pressing, Shock consolidation, Hot extrusion processes are main routes to process these brittle powders. Near full density had been achieved by these processes with the special attributes mentioned above[29].

2.4.3 Hot Densification Processes

The demand for high performance materials has resulted in the development of numerous hot consolidation approaches that can be utilized to form fully dense products Some of the well known hot consolidation techniques such as hot pressing, hot isostatic pressing (HIP), hot extrusion, and powder forging now being routinely employed to process fully dense product from advanced materials. The last two decades have witnessed the emergence of several non-conventional hot consolidation techniques such as plasma assisted sintering (PSA), dynamic magnetic consolidation (DMC), and several pseudo hot isostatic pressing techniques. Several variations based on the four conventional hot consolidation techniques have also emerged over the last two decades.

In the early phase of the development of hot consolidation , the process was restricted to exotic materials generally used in very specialized applications. As the processes became more popular, their spread into the more common materials increased rapidly. Much of the recent growth in the area of particulate materials has been spurred by the developments in the hot consolidation techniques. The modern hot consolidation techniques are currently trying to emphasize the aspect of higher productivity and consolidation of near-net shaped components.

The technique that can be classified as "hot consolidation " processes combine, simultaneous application of pressure and temperature. These processes are geared to produce almost fully dense material. This high-density result in improved material properties, which then makes the components suitable for its high-performance applications. It is clear that the property increase is quite dramatic as the material attains full density. To answer the question of where to use hot consolidation processes one should always consider the final application and the desired properties. Examples of where the use of hot consolidation techniques can be very useful includes structural components where fatigue and impact properties are extremely important or application where high strength is required at both room and elevated temperatures. It should be clear that hot consolidation techniques are very expensive as compared to press and sintered product.

The use of hot consolidation becomes extremely important in case of reactive materials that have the propensity to form surface film. Generally, sintering of these materials results in structures that exhibit prior particle boundary decoration, which is a weak link in the microstructure. To attain a disruption and good distribution of prior particle boundaries, it is simply not enough to use pressure assisted sintering. In this case it become necessary to impart significant amounts of strain and shear during consolidation processes.

2.4.3.1 Basic Of hot Consolidation Approaches

Basic mechanism of hot consolidation can be represented by the following equation[31].

$$df / dt = (1-f)\, B\, (g\gamma / x - P_g + P_E)$$

Where, df/dt is the densification rate, f is the fractional density, B is collection of parameters including diffusivity, temperature, and particle size, g is a geometric term that depends on the stages of sintering and the way of which x is measured, x is the pore diameter, γ is the surface energy, P_g is the gas pressure inside the pores, and P_E is the effective pressure.

From the above equation several important facts emerge about all hot consolidation techniques. The surface energy provides inherent sintering stress which is enhanced by the application of external pressure which goes to increase the densification rate. Gases trapped in the pores reduces the rate of densification. The rate of change of density increases with both applied pressure and the rate of mass flow. Actual densification process is also affected by stress state and the effects of stress on the various transportation mechanism. The application of pressure through gasses will be ineffective as the pressure will be distributed throughout the compact. In contrast, if the pores are closed or the pressure is applied to a pore-free container wall which contains the powder, the sinter densification process is again accelerated. However, if pressure can be transmitted to a powder mass with open pores by some granular medium (heated sand or other particulate materials) or a solid, the acceleration of sinter densification is again possible. The effective pressure is very high during the early

stages as the particles are practically in point contact. The effective stress continues to diminish and finally become the same as the applied pressure when density is 100% So the beneficial role of applied pressure during sintering becomes quite clear.

2.4.3.2 Conventional Hot Consolidation Approaches

The four most popular and conventional forms of hot consolidation that have been commonly successful are hot pressing, hot isostatic pressing, forging and extrusion. Figure 2 7 shows the basic schematic diagram of the four processes .

2.4.3.2.1 Uniaxial Hot Pressing

This is the simplest form of hot consolidation process that is extensively used to densify high temperature materials. In its simplest form, the processes of hot pressing consist of loading loose powders of the material to be consolidate into a graphite die. The die is usually of a simple cross-section. The graphite mold is generally is lined with a non-reactive carbonaceous material to reduce reaction between the powder material and the die. Other die material used are refractory metals and alloys and some ceramics. The pressure applied is uniaxial in nature and is applied to the punches through a ram. The temperature capability of this process is very high and can be in the range of 2373 K. The pressure is usually on the low side and is limited by the strength of the graphite. Typically, pressure used are in the range of 25 to 40 Mpa. The pressure applied is unixial, but the die wall constraint creates a radial

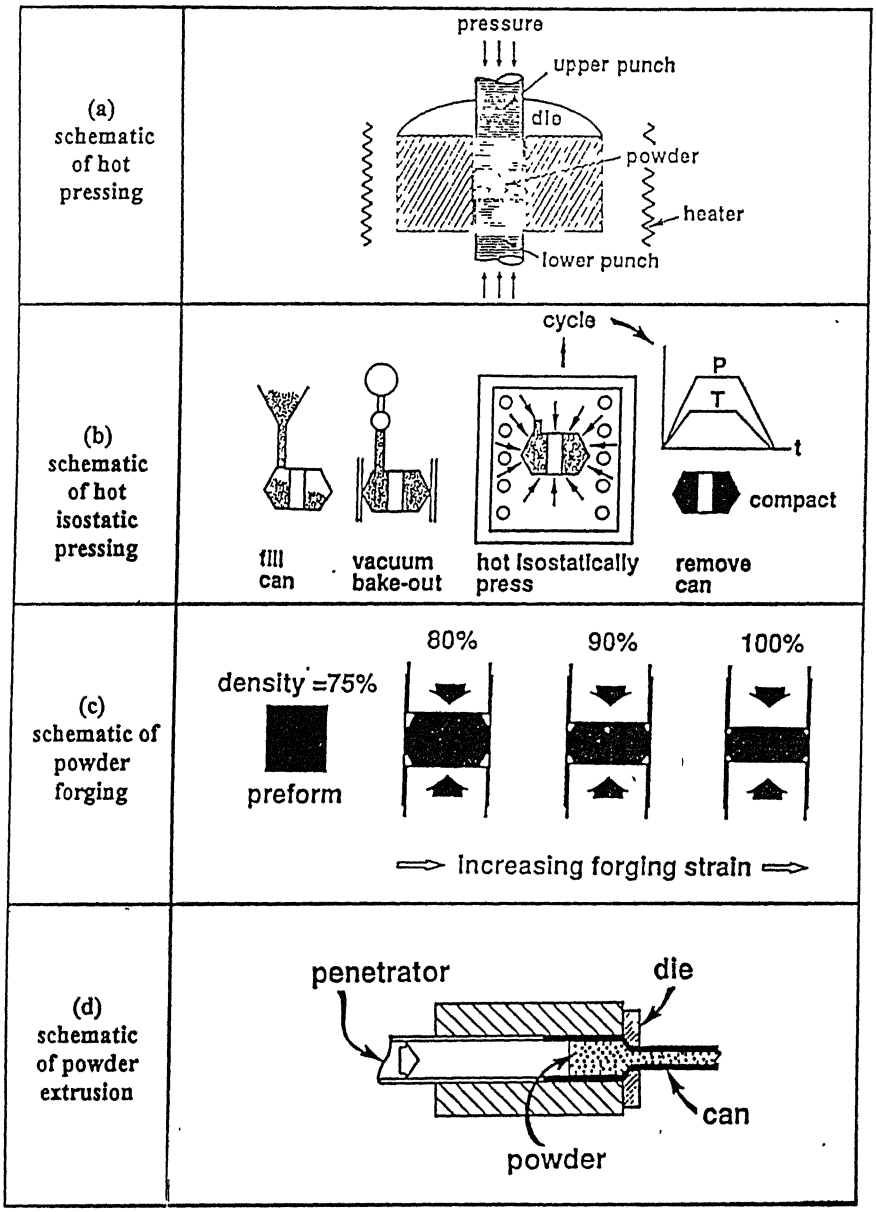

Fig 2.7 Schematic of four conventional hot consolidation processes

pressure. Thus, a small amount of shear is imparted to the powder particle in this process. The process is slow and has poor control on the heating and cooling rates due to the mass of the tool. The shape that can be produced are also very simple. Hot pressing is extensively used in processing high temperature materials, exotic material composition, a variety of different composites with reinforcing agents in the form of particulates, platelets, whiskers and fibers. Some of the commercial application include metal-bonded diamond cutting tools, sputtering targets, TiC-Fe composites, and a new class of composites known as micro-infiltrated macro-laminated composites.

2.4.3.2.2 Hot Isostatic Pressing (HIP)

This is the most popular hot consolidation technique that is in commercial use. The process starts with the selection of a container that will encapsulate the powder that is to be consolidated. The container is generally made from a low carbon steel material, stainless steels, titanium, copper, and niobium based alloys. Typically the can is sealed on one side and the powder is filled in through the other side. Once the can is filled with powder, the can is evacuated through a top stem. The powder is heated while a dynamic vacuum is being continuously pulled. This ensures proper degassing of the powder particles. Ones the degassing is complete, the stem is crimped and the powder is vacuum encapsulated. The powder filled, vacuum encapsulated can is then introduced into HIP chamber. The chamber is properly secured, pressurized, and heated. High pressure gas is the medium that is reasonable for the transfer of heat and pressure to the container wall

which then transfer it to the powder inside. Temperature of 2373 K and pressure of 250 Mpa have been used in this process. The pressure that is applied is hydrostatic in nature. The process does not result in induced shear. Once the consolidation process is complete, the temperature and the pressure in the HIP chamber is allowed to decrease to normal level. Then different processes including, machining, grinding, and chemical leaching remove the container material. The process is quite slow and expensive. It is also important to consider the metallurgical aspects of possible reaction between the can material and the powder. The process is suitable for large components. The process has been extensively used to consolidate a variety of different materials including tool steel, superalloys, intermetallic compounds and ceramics.

2.4.3.2.3 Forging

This is the oldest form of metal working technology. One of the oldest P/M relics, the Iron Pillar in Delhi is believed to have been produced by hot forging of sponge iron pieces. The modern era of powder forging was rekindled around the middle of this century when various components such as water pump gears, materials for nuclear powder generation, feed pawl for antiaircraft guns, etc., were processed by powder forging. Forging is an elevated temperature, high strain rate deformation process. The process is also used in the slow strain rate mode to superplastically form fine grained material. There are basically two different forms of powder forging:

1. Hot powder upsetting in which the preform experiences a significant amount of lateral material flow .

2. Hot re-pressing where material flow in the lateral direction is small and the densification is mainly in the pressing direction.

In the first process, extensive lateral flow of material occurs creating a stress state around the pore which is a combination of normal and shear stresses. Thus a spherical pore becomes flattened and elongated, and the shearing causes the collapsed pore surfaces to rub across each other and form stronger bonds compared to a simple pore collapse with no relative motion or pore surface elongation. In contrast during repressing there is very little shear and the pores are not significantly elongated. The process does not attain optimal properties due to the reduced interparticular movement. Fig 2.8 shows a schematic of the powder repressing and powder forging process.

2.4.3.2.4 Extrusion

Powder extrusion provides an alternative route for processing materials to almost full density. This is a technique that is often used for producing long bars or rods of high performance materials. The process is suitable for producing shapes that have a uniform cross-section over a large length. The cross sections are usually simple, such as squares, rectangles, circle, etc. The process is also capable of co-extrusion, which results in one material forming a layer on another over the entire length of the final extrudet product. The process of powder extrusion is carried out at a elevated temperature, high strain rate, and high stress. The major advantage of this process is the very high shear and deformation that the powder particles are subjected to during the process This high shear deformation helps in breaking up oxide skin, collapses pores and

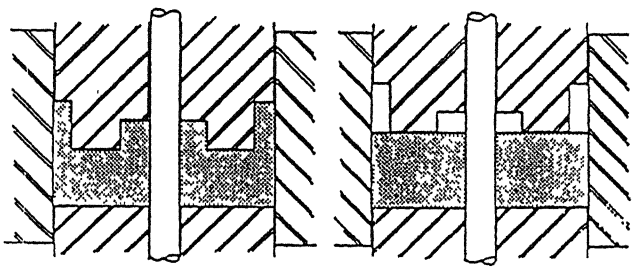

Fig 2.8 Comparison of a) powder repressing and b) powder forging.

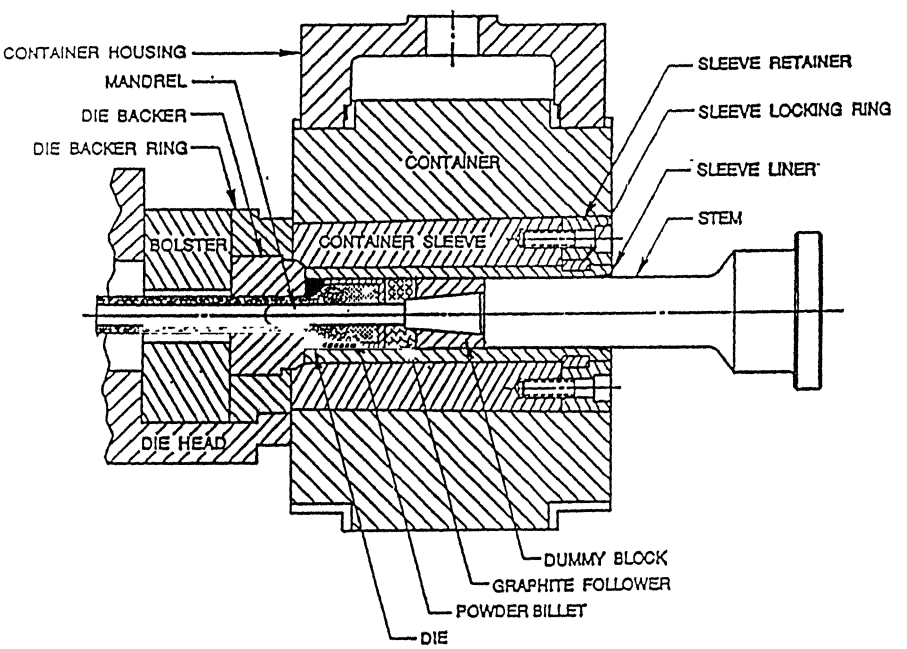

Fig 2.9 Detailed schematic diagram of an extrusion press

creates material bonds, and promotes nascent particle-particle contact. The process gained popularity in the P/M community and has been used to consolidate numerous high performance materials such as nickel and iron aluminides, refractory metals and alloys, and large number of ceramics.

The extrusion constant C, the extrusion force F, cross-sectional area of the feed material A, and the reduction ratio are related by the following equation.

$$F = C A \ln (R)$$

The extrusion constant C combines several parameters such as stress, friction and redundant work into one. The extrusion temperature, lubrication, and the material properties, all have a bearing on the extrusion process. A schematic diagram of an extrusion press is shown in Fig 2.9. Extrusion of P/M materials can be accomplished by hot extruding pre-compacted and sintered material or going through the route of canning powders (in vacuum) and hot extruding the powder filled can.

2.4.3.3 Non-Conventional Hot consolidation Process

The limitations of the conventional techniques have resulted in the rapid proliferation of some non-conventional hot consolidation processes. These processes try to increase production rate, reduce sample preparation time, and overcome the shape limitation of conventional processes.

Some of them are Q-HIP(Quick HIP), ISP(Isostatic High Rate Pressing), PAS (Plasma Activated Sintering), DMC (Dynamic Magnetic Consolidation).

Q-HIP is the modification of hot isostatic pressing. In ISP pressure transmitting medium is molten glass. PAS is usually carried out in a graphite die into which the powder is poured. Uniaxial pressure is applied to the powder at the start. An external power source first provides a pulsed plasma to activate the powder surface and then switches to resistance heating for densification. It is postulated that electrical discharge, resistance heating, and mechanical pressure are the three factors in the PAS process that actually contribute to densification. The process DMC is a relatively new consolidation technique where primarily pressure is generated from pulsed electromagnetic fields. The powder is enclosed in a confining conductor and placed in the center of the compactor coil. The current in the compactor coil generates a magnetic field which produce magnetic pressure on the powder material. The pressure applied is radial in nature.

CHAPTER THREE

EXPERIMENAL PROCEDURE

3.1 STARTING MATERIAL

Iron and iron-aluminide powders were used as starting materials.

3.1.1 Iron Powder

Electrolytic iron powder of purity > 99 0% supplied by Sudhakar Products, Mumbai, was used. Characterization of the powder shape, was done in a previous study[21], Iron particles are shown to be of somewhat round shape. Size distribution of iron powders in histogram is shown in Figure 3.1. As shown, iron powder particle size lies in narrow range of 80 to 110 μm. BET surface area measurement results as obtained from COULTER (machine to measure surface area), gives specific surface area of the iron powder as 0.538 sq.m/g.

3.1.2 Iron Aluminide Powder

As a starting material Fe_2Al_5-$FeAl_2$ phase mixture was used. The X-ray diffraction result obtained from the starting iron aluminide powder is shown in the Figure 3.2. Which clearly indicates the presence of Fe_2Al_5-$FeAl_2$ in the starting material. Iron aluminide powder was produced be mechanical alloying method.

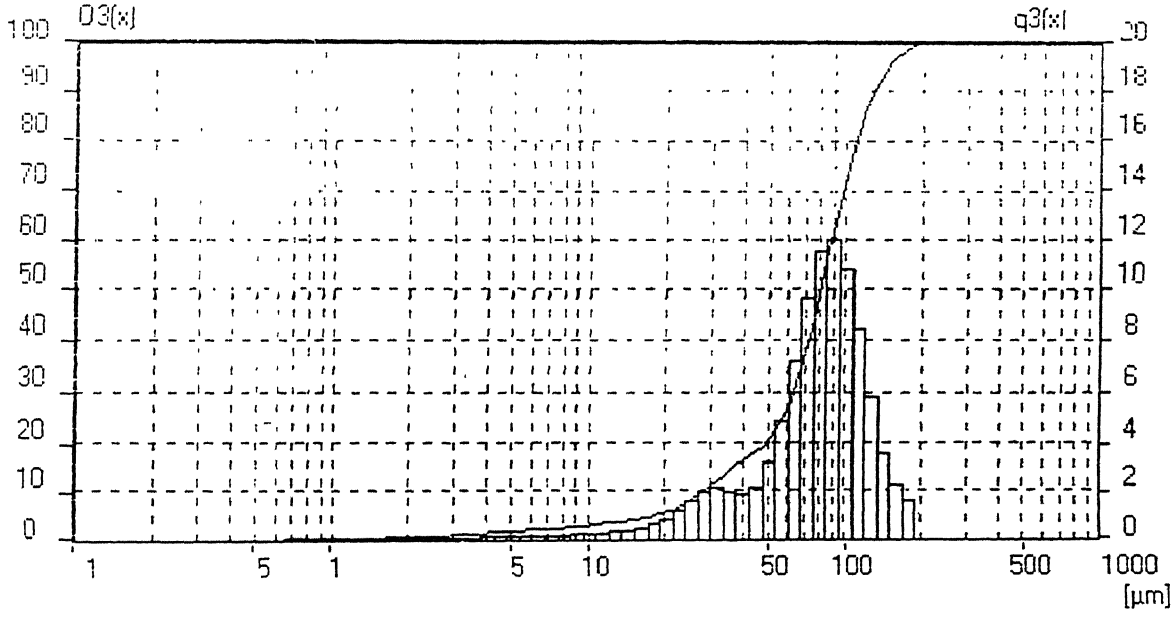

Figure 3.1: Histogram showing particle size distribution of iron powder.

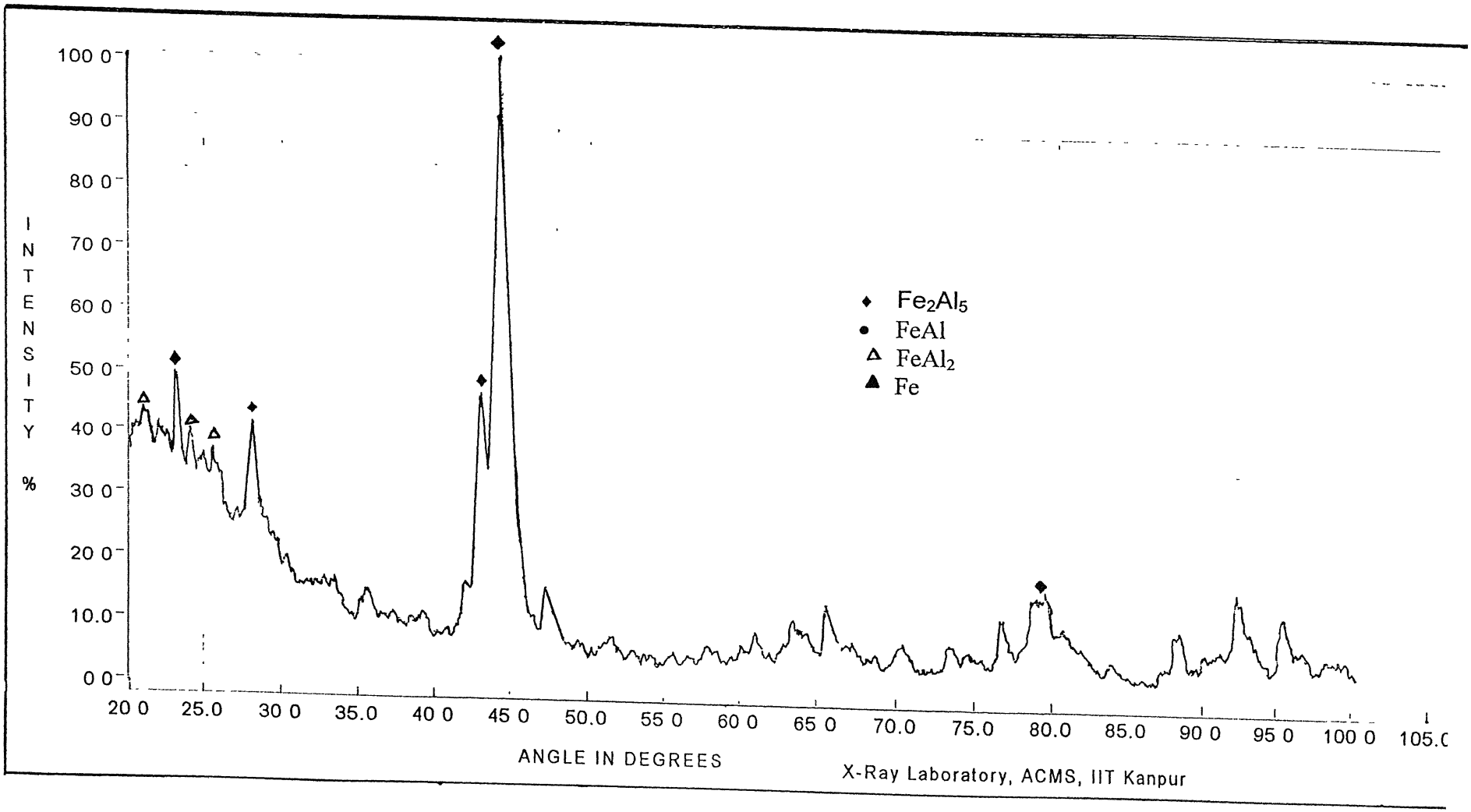

Fig 3.2 X-ray diffraction results of Iron Aluminide powder.

The particle size distribution of iron-aluminide powder is shown in Figure 3.3. According to the histogram shown in Figure 3.3 iron-aluminide powders were distributed mainly in the 70 t0 100 μm size ranges. BET specific surface area for aluminide powder used is 0.242 sq.m/g as obtained from COULTER' surface area results .

3.2 REDUCTION OF IRON POWDER

The iron powder available supposed to have some oxide impurities. These impurities may affect densification during sintering by hindering the diffusion process. Therefore reduction of iron powder was thought necessary to clean the powder. The set up used for reduction is schematically shown in Figure 3.4. Hydrogen gas was used as the reducing agent. The iron powder was put in a quartz glass tube, closed at one end. Hydrogen inlet and outlet both were on the same side for better thermal and reduction efficiency. Reduction was done at 500^0C for one hours. Hydrogen atmosphere was maintained during cooling of reduced powder to 50^0C. This reduced iron powder was used in further experiments directly.

3.3 HOT PRESSING OF IRON –IRON ALUMINIDE POWDER MIXTURE

In Hot pressing temperature and pressure is applied simultaneously; that is schematically shown in figure 3.5.

Hot pressing experiments were done in the hot press of Dr. FRITSCH K. G.,West Germany. Powder mixture was filled in 10mm. diameter graphite die. It was then loaded with graphite punch. A

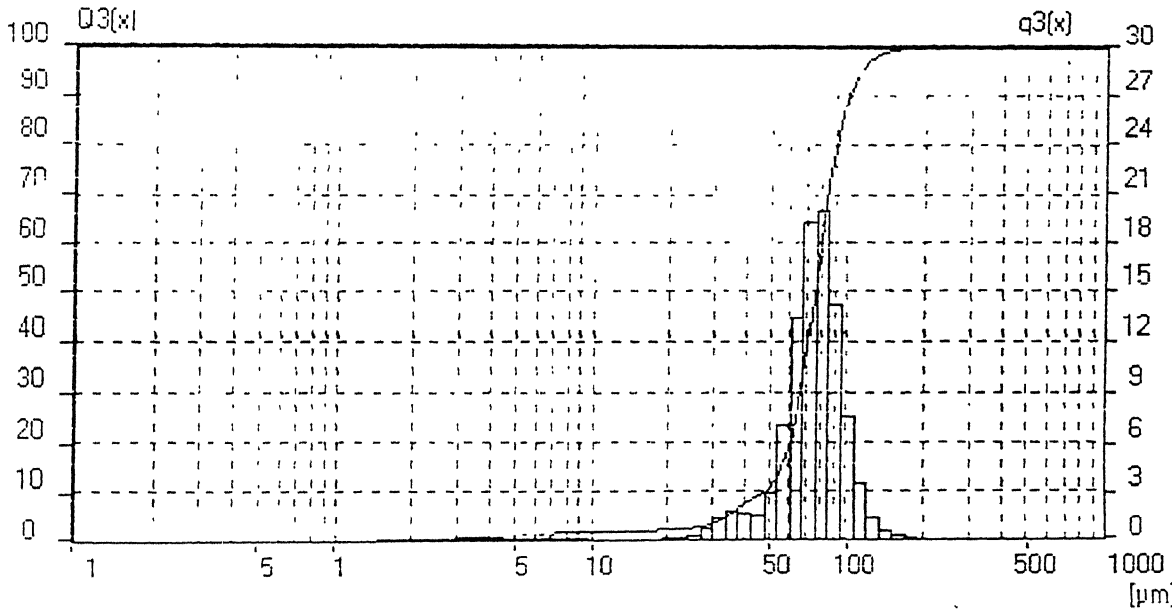

Figure 3.3 Histogram showing particle size distribution of iron aluminide powder

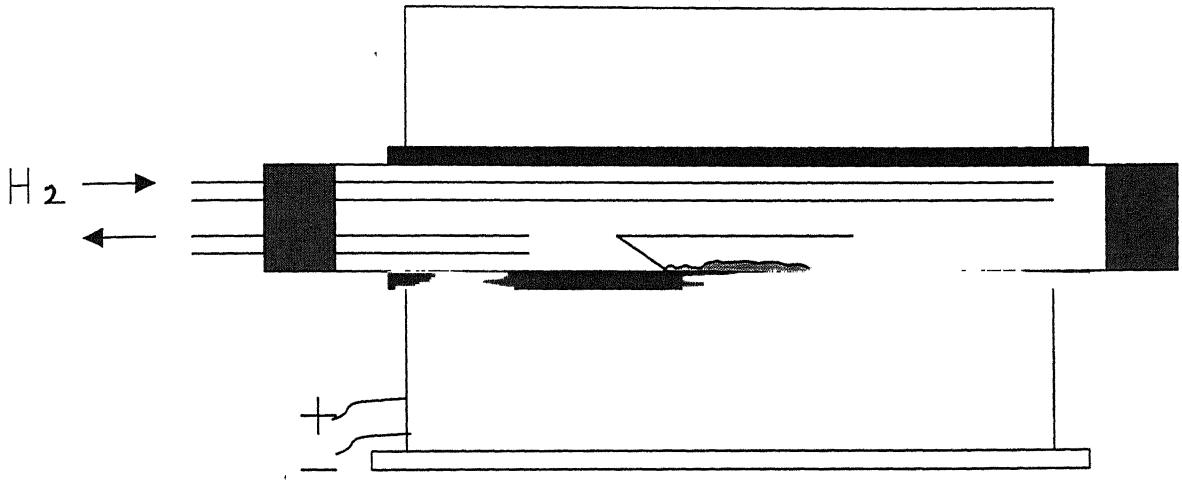

Fig 3.4 Schematic diagram of the apparatus used to reduce iron powder.

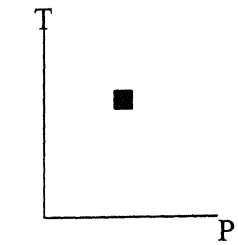

full densification cycle

Figure 3.5: Schematic diagram of full densification method.

schematic sketch of the die is shown in Figure 3.6. The various steps involved in the hot pressing procedure are as follows:

1)Powder is placed in the die mold.

2)The mold is heated by resistance heating to a predetermined temperature.

3)The powder in the die cavity is then pressurized.

4)The temperature is steadily increased during compaction until a maximum required temperature is reached.

5)Compaction pressure and temperature are maintained for dwell time.

6)The mold is cooled slowly, under pressure, to ambient temperature

The hot pressing was done at four temperatures of 800°C, 850°C, 900°C and 950°C. The temperature was continuously monitored by chromel-alumel thermocouple inserted into the graphite die wall. It took 1 hour for one hot pressing including 20 minutes holding time at the hot pressing temperature.

A schematic sketch depicting hot pressing set-up is shown in Figure 3.7.

Samples containing 20%, 30%,40%and 50% Fe were prepared for hot pressing in the temperature mentioned above. Two sets of sample was prepared, one for microstructure analysis and another for compression test.

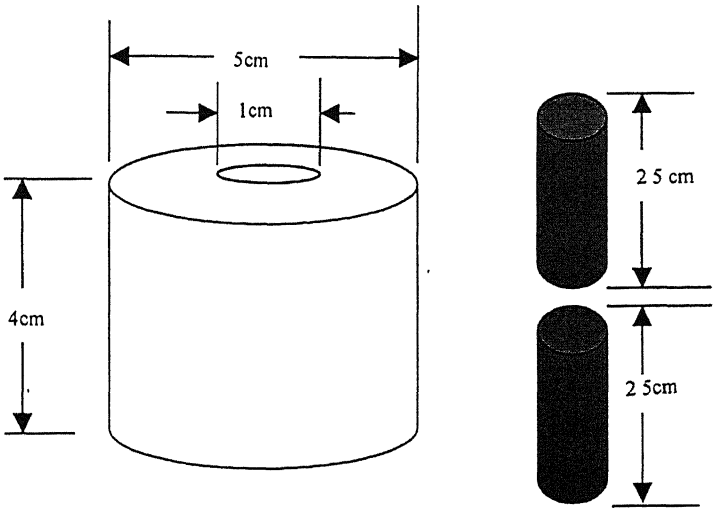

Fig 3.6 Schematic diagram of die and puuch.

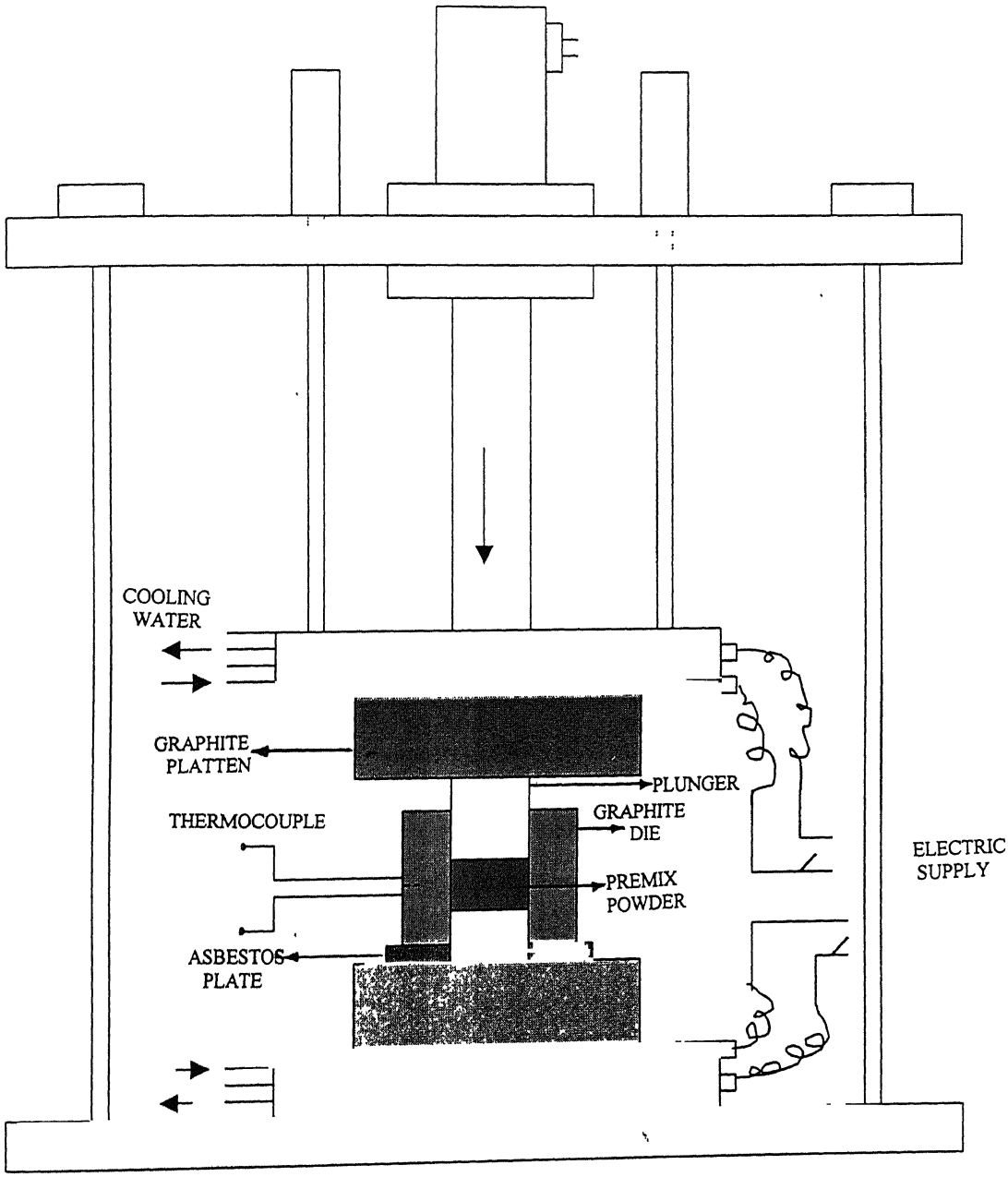

Figure 3.7 : Schematic diagram of the hot pressing unit used

3.4 CHARACTERIZATION OF HOT PRESSED SAMPLES

3.4.1 X-ray Diffraction Analysis

X-ray analysis of powders and hot pressed samples was done on ISO-DEBYEFLEX 2002 with Cu-Kα radiation . The 2θ values were obtained directly through X-ray diffraction. These 2θ values were compared with standard 2θ values given in JCPDS Powder Diffraction Data files for identification of the phases.

3.4.2 Scanning Electron Microscopy

Powders and hot pressed samples were observed under JEOL JSM 840A scanning electron microscope (with EDAX facility) at an operating voltage of 15 kV.

The hot pressed samples for SEM were prepared by first polishing the samples, cut by diamond cutter, on SiC emery paper of grades 180, 320, 400, 600 followed by coarse and fine wheel polishing alumina powder suspension in water. An etchent of 10%HNO_3 + 10%HF + 80% H_2O (by volume)[33] was used to reveal the details of microsrructure.

3.4.3 Optical Microscopy

Optical micrograph was taken for the etched samples at magnification 100X, 200X, 500X, 1000X.

3.4.4 Density Measurements

Densities of samples were measured by dividing weight by the volume of samples. The oil impregnation method was used to measure density. In oil impregnation method, samples were impregnated with xylene under vacuum and the following formula was used for determining the sintered density.

Sintered density = a / (b-c)

a= weight of compact in air, b= weight of xylene impregnated compact in air, c= weight of xylene impregnated compact in water

% Porosity = (theoretical density – apparent density)/ theoretical density.

Volume of open pores = (b-a) / 0.863.

Volume fraction of open pores = (b-a) / [(b-c) x 0.863)]

3.4.5 Hardness Testing

Microhardness measurements were done on hot pressed samples using Leitz Miniload Microhardness Tester.

3.4.6 Compression Testing

Compression tests were carried out using two machines. The first one is MTS machine with cross-head speed of 0.5mm/min. The second one is RIEHLE compression testing machine of 135000-kg .The dial that is used is of 25000-kg with a list count of 50 kg. For compression testing diameter of the specimen should be equal to its length[32]. The compressive strengths were calculated from the load applied divided by the final area of the compacts.

CHAPTER FOUR

RESULTS AND DISCUSSION

4.1 HOT CONSOLIDATION OF THE IRON ALUMINIDE-IRON POWDER MIXTURES

4.1.1 General Considerations

As depicted in Figure 2.2, the binary Fe-Al phase diagram shows the existence of several iron aluminides, namely Fe_3Al, FeAl, $FeAl_2$, Fe_2Al_5 and $FeAl_3$ that form in the Fe-Al system. These compounds possess their own crystal structures and specific properties. The general feature of their deformation behaviour is that as the percentage of Al in them increases their high temperature deformability decreases Therefore, it is very difficult to process the high Al content Fe-Al intermetallics, such as $FeAl_3$, Fe_2Al_5, $FeAl_2$ or their two-phase alloys by the conventional ingot metallurgy (I/M) routes. They may however be processed by various powder metallurgical (P/M) routes such as reactive sintering and/or hot consolidation methods involving pre-alloyed powder(s).

The wet chemical analysis from the starting iron aluminide powder showed that it contained ~ 51 wt % Fe and ~ 49 wt % Al implying that the starting material is expected to be a phase mixture of Fe_2Al_5 and $FeAl_2$. The X-ray diffraction results from the starting powder are shown in Figure 3.2. These results confirm that the starting material was indeed a mixture of Fe_2Al_5 and $FeAl_2$.

In a previous study by Yadav, efforts were made to consolidate the given iron aluminide powder by (a) sintering of iron aluminide or iron-iron aluminide powder compacts, (b) high-temperature densification rolling of sintered porous compacts made from iron aluminide or iron-iron aluminide compacts and (c) hot pressing of iron aluminide powder or iron-iron aluminide powder mixtures under a limited set of temperature-pressure conditions. Among these processing routes, the routes involving sintering and that involving hot densification rolling were not found to be effective. In contrast, the reactive sintering route is not very suitable as the heat of reaction during reactive sintering in Fe-Al system is not sufficient to continue a self-sustaining reaction. Another approach is involves with the addition of softer phase like either Al or Fe in the original powder and carrying out the hot pressing of the powder mixture. However, Al is not a suitable addition due to its swelling tendency at high temperatures. So in present work Fe was added as a softer phase. Fe was added in different proportions. In previous work conventional route was followed i.e. cold compaction and then sintering to a very high temperature but this approach did not produced satisfactory result. So in present wok uniaxial hot-pressing was followed to consolidate the powder. The iron powder was added in aluminide powder in the proportion of 20wt%, 30wt%, 40wt% and 50wt%. And hot consolidation of these powder mixtures was done at temperatures 800, 850, 900, 950^0C.

4.1.2 Density, Inter-connected Porosity and the Relative Density of hot pressed Iron Aluminide Compacts

As given in chapter 3, density of the hot pressed samples was measured by the displacement method using Archimedes principle. Fig 4.1 shows the variation of density of the hot pressed iron aluminide compacts with increase in hot pressing temperature for powder mixtures of different Fe%. These plots clearly indicate that the density of hot pressed compacts increases with (a) hot pressing temperature and (b) wt % of Fe in the iron aluminide-iron mixture.

The presence of iron in the iron aluminide-iron mixture effects the densification of compacts in two ways: (a) the density of iron being higher than that of iron aluminide, the presence of iron in the powder mixture would increase the density of the hot pressed compact and (b) iron being the softer phase would assist the densification of the compact and as the volume fraction of the softer phase increases the density of the hot pressed compact would increase. In order to separate the effect of these two factors, the data on density of hot pressed aluminide compacts were used to obtain the increase in density ($\Delta\rho$) as a function of Δ wt % Fe of powder mixtures for all the hot pressing temperatures, 800°C, 850°C, 900°C and 950°C, used in the present study. The plots between $\Delta\rho$ and Δwt % Fe are shown in Fig 4.2. It may be seen that the slope of the increases as the wt % iron increases for all the hot pressing temperatures.

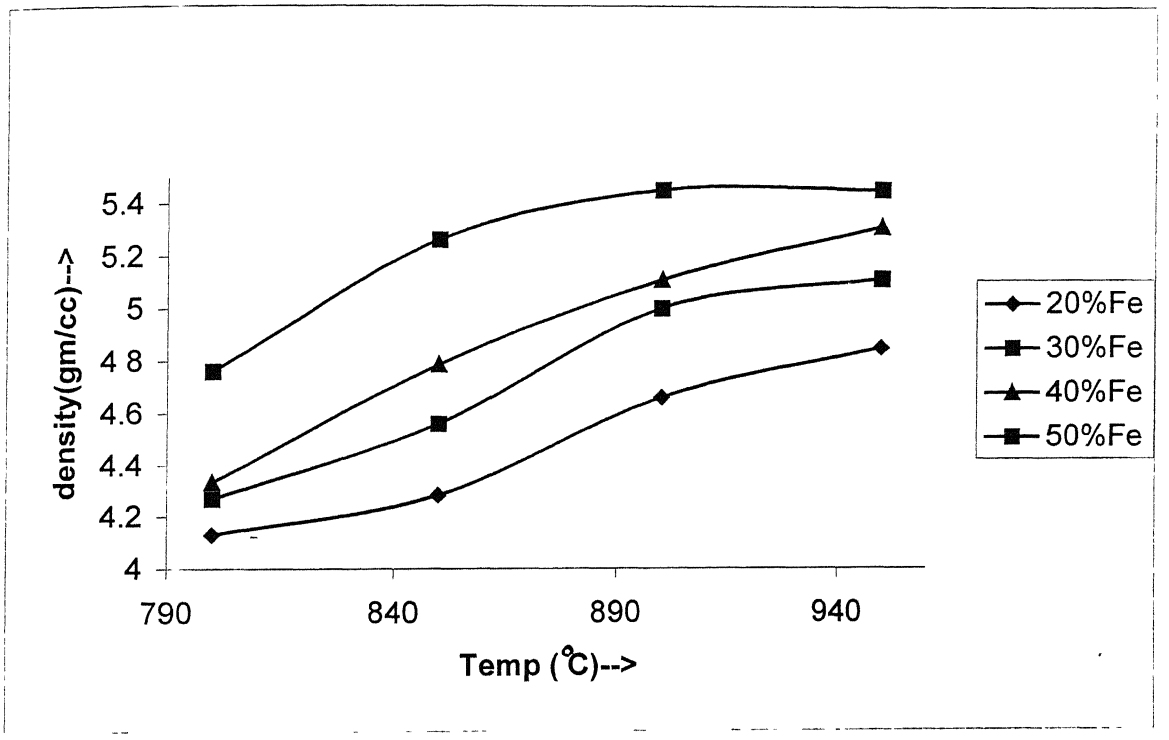

Fig 4.1 plot showing variation in density of the compacts with temperature for samples containing different Fe%.

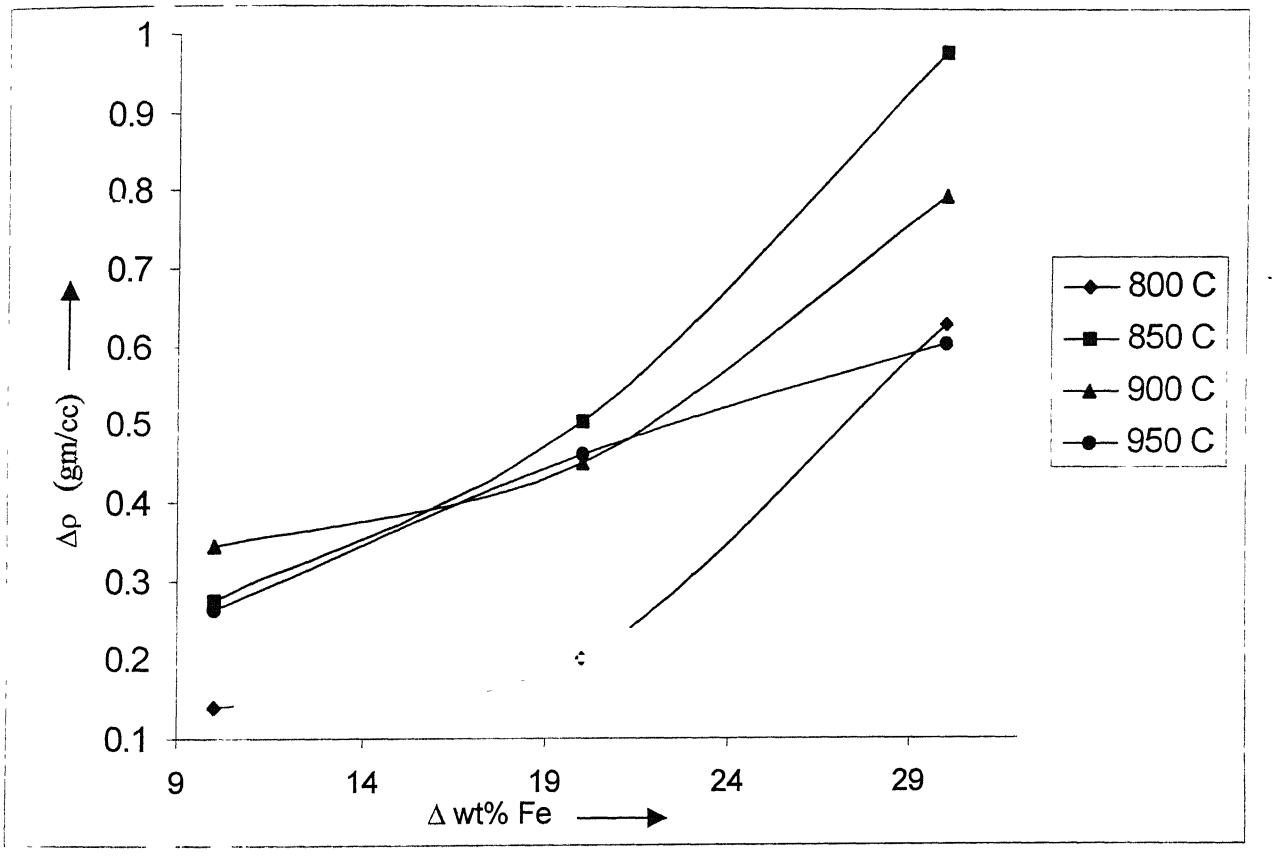

Figure 4.2 Plot showing variation in $\Delta\rho$ with Δ wt% Fe at different hot pressing temperature.

However, as the hot pressing temperature increases the rate of change of the slope decreases.

It is worth noting that if the density of hot pressed compacts increases due to the heavier constituent (iron) alone and the presence of soft phase has in the mixture has little role to play in the consolidation behaviour of the powder mixture, one would predict a some what linear behaviour of $\Delta\rho$ versus Δwt % Fe plots, i.e. plots having the constant slope. The increasing slope of the plots with increasing iron content at the hot pressing temperatures of 800°C to 900°C therefore does indicate that the consolidation of iron aluminide-iron powder mixtures is assisted due to the presence of softer iron particles. This observation, however, can not be readily made for the hot pressing temperature of 950°C, the temperature at which iron particles do not retain their identity as iron particles and quickly transform to iron aluminide due to the faster diffusion occurring in the system.

Assuming homogenization of the compact by the diffusion of the entire iron into iron aluminide, the additions of 20 wt%, 30 wt %, 40 wt % and 50 wt % of iron in the iron aluminide - iron powder mixtures, the resultant hot pressed compacts would comprise of (a) $FeAl_2$ and FeAl (for 20 and 30 wt % Fe respectively) and (b) FeAl (for 40 and 50 wt % Fe respectively). Since the lattice parameters of these phases of nonstoichiometic compositions are not readily available, estimation of the theoretical density of the hot pressed compacts is impractical. However,

the data for the density measurement were used to estimate the % of open porosity present in the compact using the following formula

% open porosity = [volume of open pores/volume of the compact] x 100

The estimated open porosity in compacts of different wt % Fe hot pressed under different temperatures is shown in Table 4.1. It is seen that the minimum of ~ 0.5% open porosity was found to be present in the hot pressed iron aluminide compacts prepared under the consolidation conditions studied in the present investigation.

As shown by the microstructures of the hot pressed samples (Section 4.3), insignificant porosity was observed in them. In the absence of the theoretical density data of the hot pressed sample, the density levels obtained in samples hot pressed at 950°C were assumed to be 99% of the theoretical density and the relative density of the compacts were estimated. Fig 4.3 shows the distribution of relative density of the powder mixtures of different iron contents hot pressed at different temperatures. It is clear from this figure that in each case the relative density value increased with increase in hot pressing temperature. It is also seen that the mixtures containing 50 wt % Fe became nearly dense at the hot pressing temperature of 900°C itself.

Table 4.1 Percentage of open pores in compacts made from Iron-Iron aluminide powder mixture in different hot pressing temperature.

wt %Fe	Hot pressing temperature (^{0}C)			
	800^{0}C	850^{0}C	900^{0}C	950^{0}C
20	11.60	7.55	1.70	0.96
30	12.01	3 62	1.10	0.93
40	7.86	2.80	1.05	0.98
50	10.07	4.53	1.03	0.53

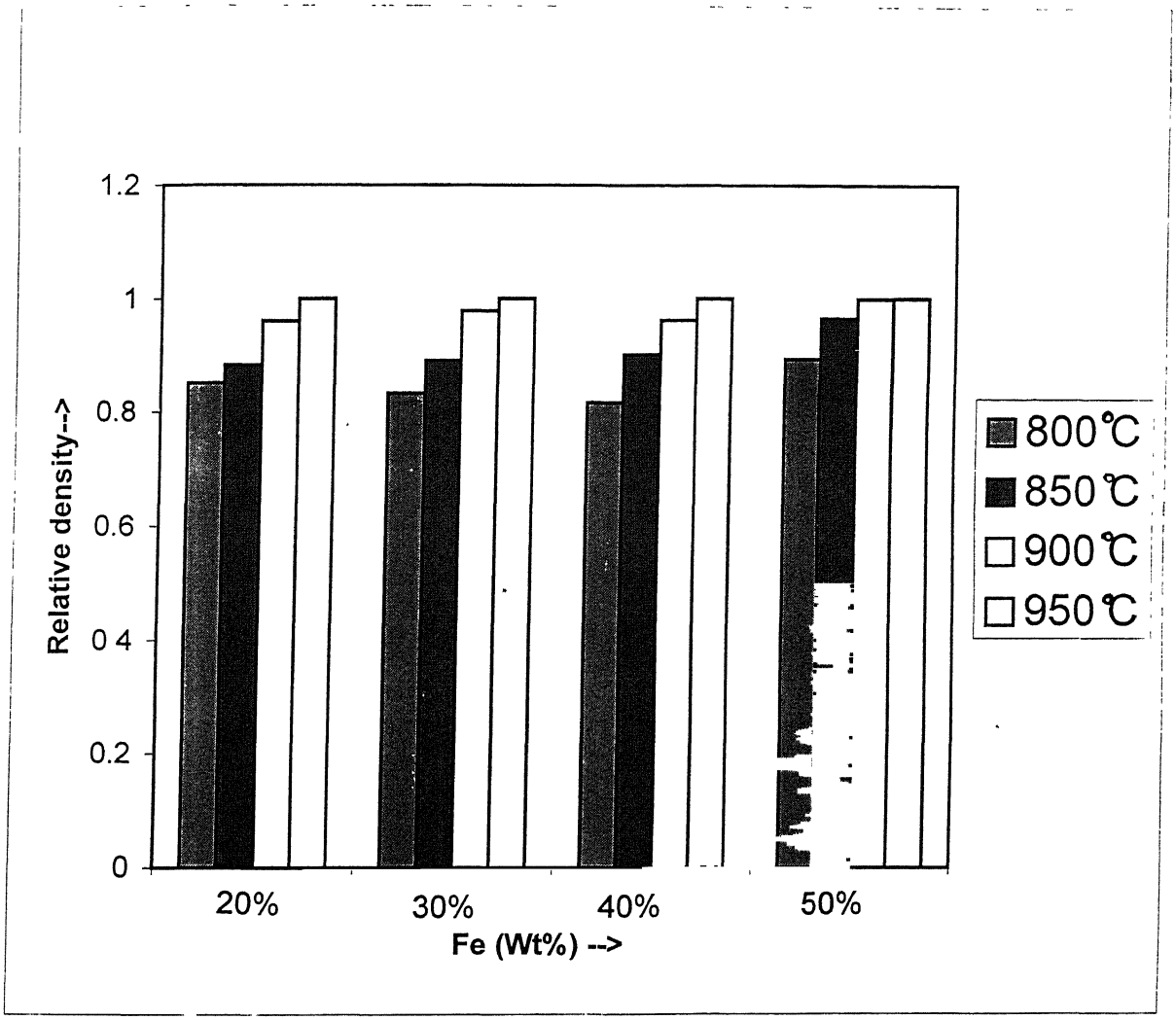

Figure 4 3 Bar chart showing variation in relative density with hot pressing temp for compact containing different Fe%

4.2 IDENTIFICATION OF IRON ALUMINIDES FORMED DURING HOT PRESSING

4.2.1 The possible phases in hot pressed products.

As iron is added in Fe_2Al_5-$FeAl_2$ phase mixture, the final composition shifts towards the iron rich side of the Fe-Al phase diagram. Assuming that the complete homogenization takes place, the proposed phases can be determined straight away from the composition. Addition of 20 wt% iron in Fe_2Al_5-$FeAl_2$ results in final composition of 57 at% Al and 43 at% Fe, which fall in $FeAl_2$–FeAl region of the phase diagram. Addition of 30 wt% iron corresponds to the final composition of 52 at% Al and 48 at% Fe, which also falls in $FeAl_2$-FeAl region of the phase diagram. On the other hand, addition of 40 wt% and 50 wt% correspond to 46.2 at% and 40.13 at% Al respectively. And these two compositions belong to single phase FeAl region. The compositional regions of iron aluminide - iron mixtures used for the hot pressing are shown in Fig 2.2.

4.2.2 Identification of phases in the hot pressed products.

Phase identification in hot pressed samples was done using the X-ray diffraction technique Characteristic plots of a few hot-pressed samples are shown in Fig 4.4 to Fig 4.12. In order to identify the phases in these samples standard diffraction data was used. The standard diffraction data for all the five intermetallic phases was taken from JCPDS files. Diffraction angles i.e. 2θ for the first five highest intensity peaks of all the Fe-Al

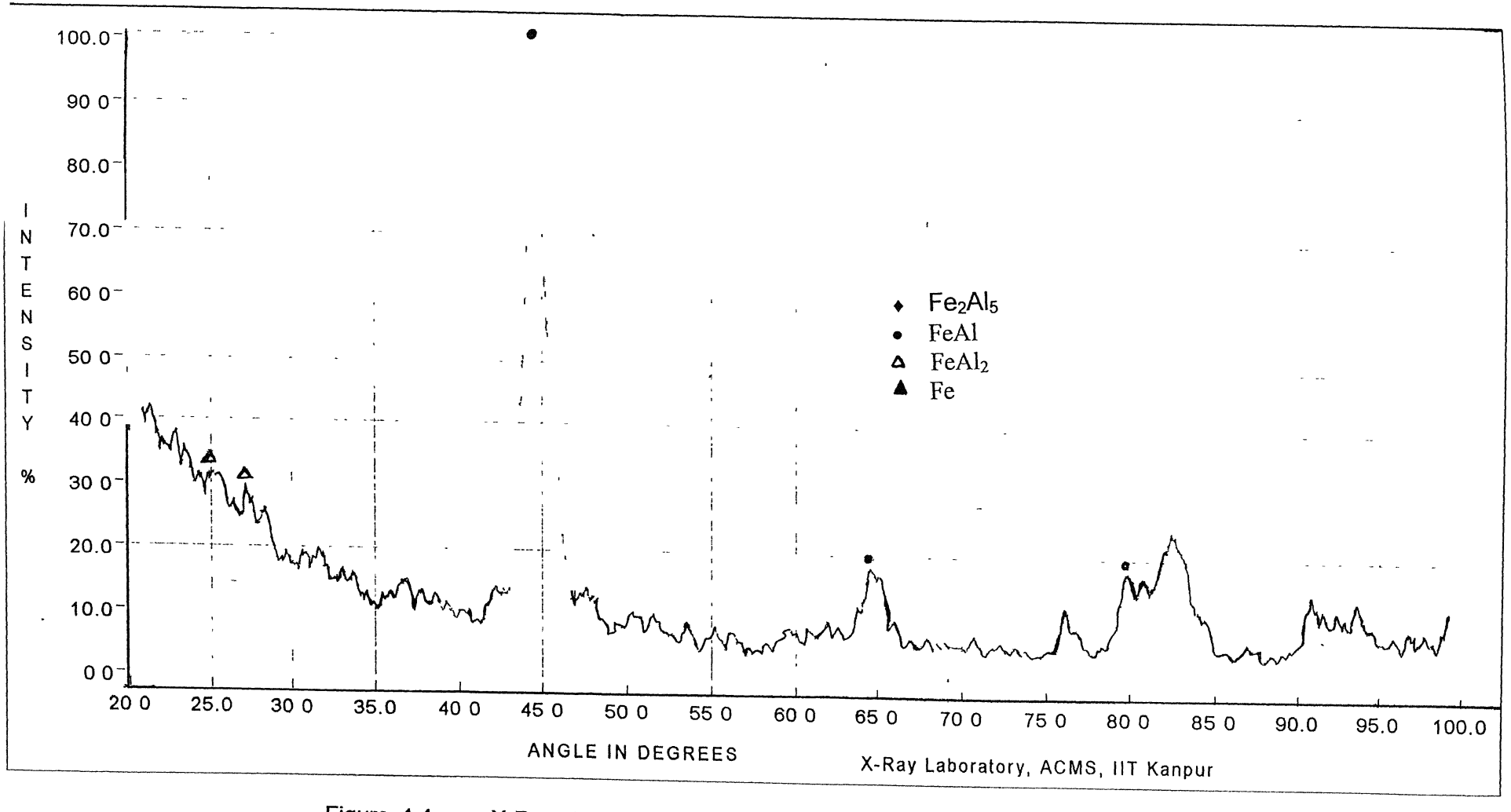

Figure 4.4 : X-Ray diffraction results of iron-iron aluminide sample Hot pressed at 800^0C and containing 20%Fe by weight.

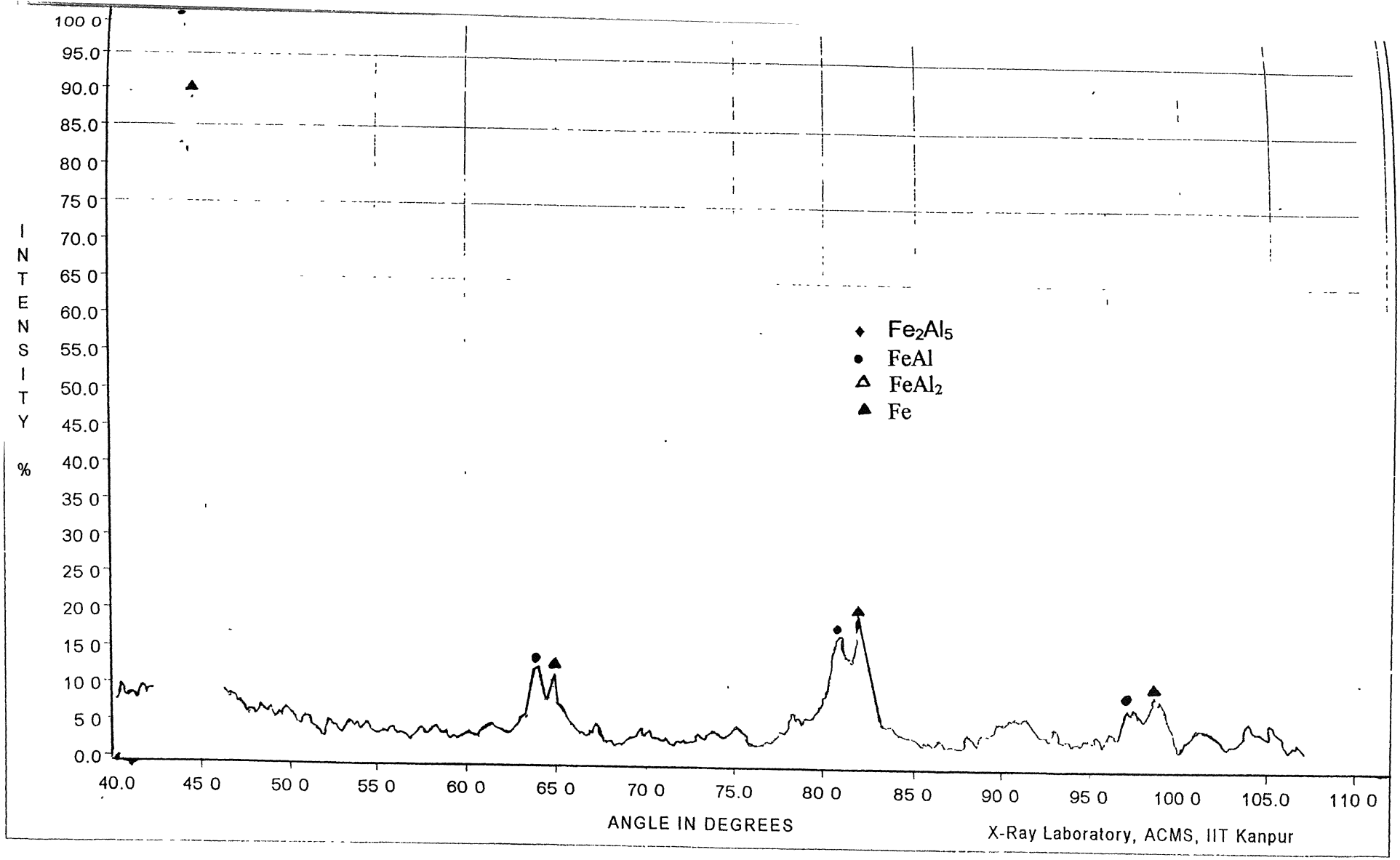

Figure 4.5 · X-Ray diffraction results of iron-iron aluminide sample Hot pressed at 800^{0}C and containing 50%Fe by weight

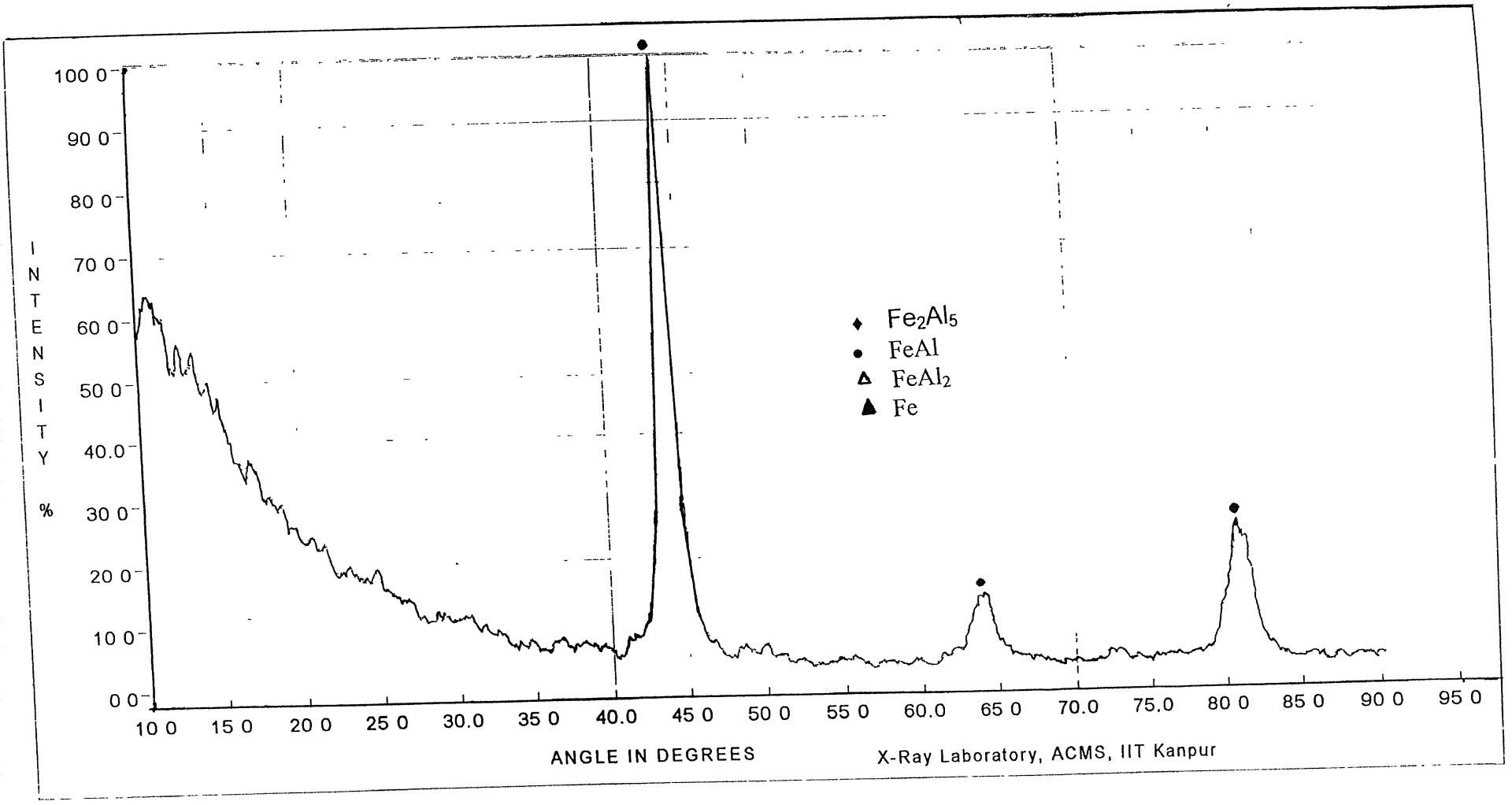

Figure 4.6 : X-Ray diffraction results of iron-iron aluminide sample Hot pressed at 850^0C and containing 40%Fe by weight

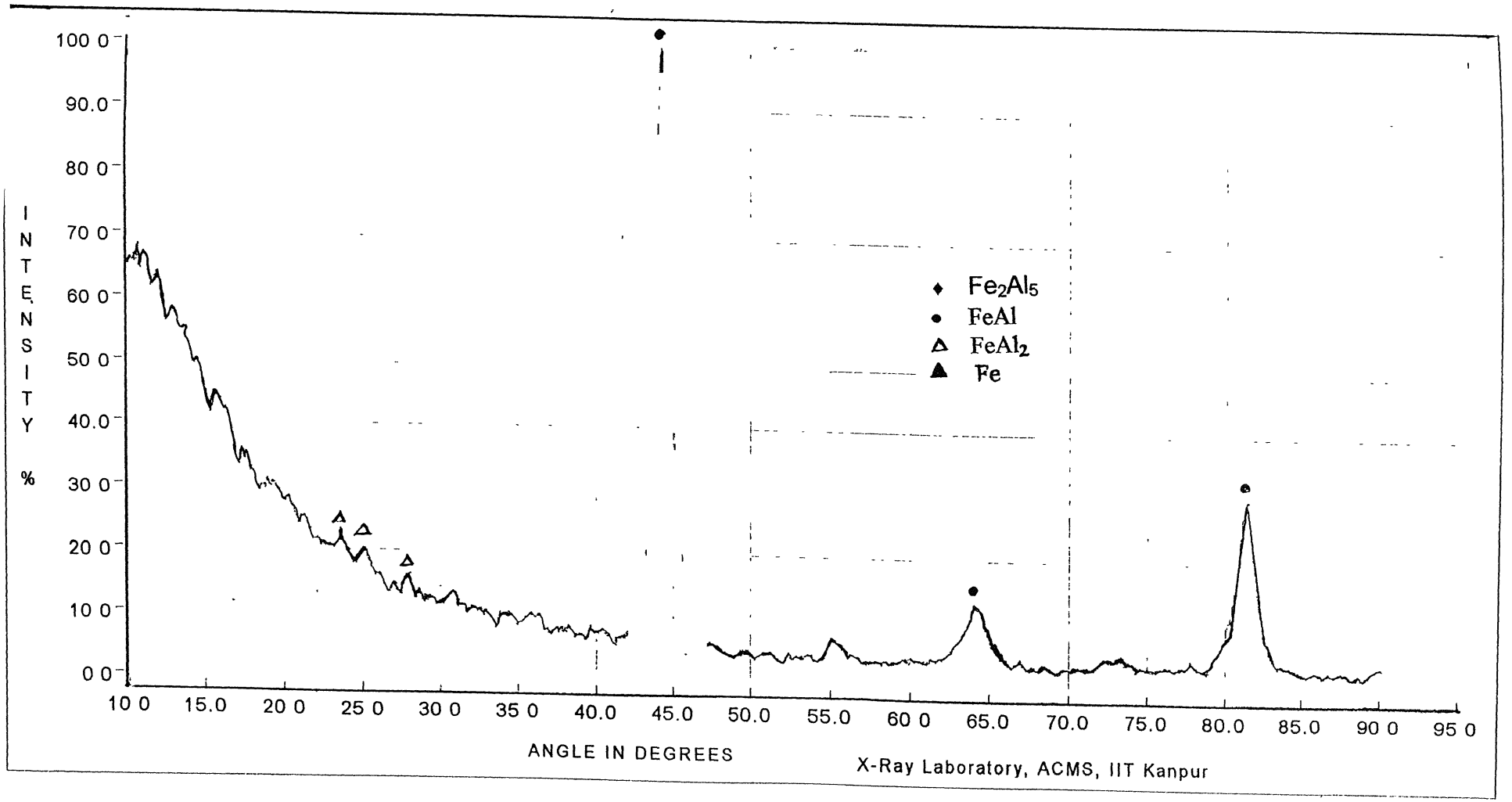

Figure 4.7 : X-Ray diffraction results of iron-iron aluminide sample Hot pressed at 900^0C and containing 30%Fe by weight

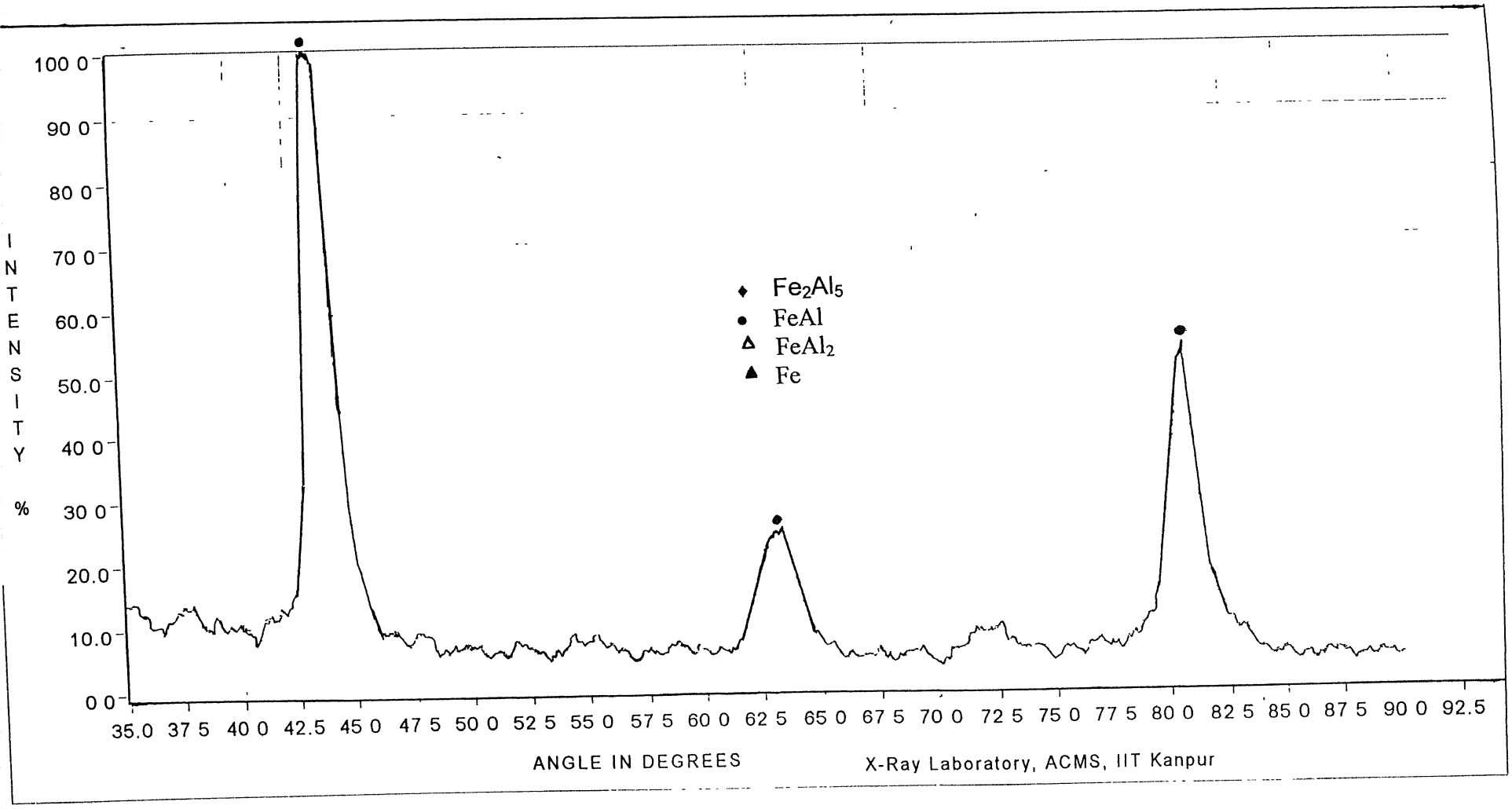

Figure 4.8 · X-Ray diffraction results of iron-iron aluminide sample Hot pressed at 900^0C and containing 40%Fe by weight

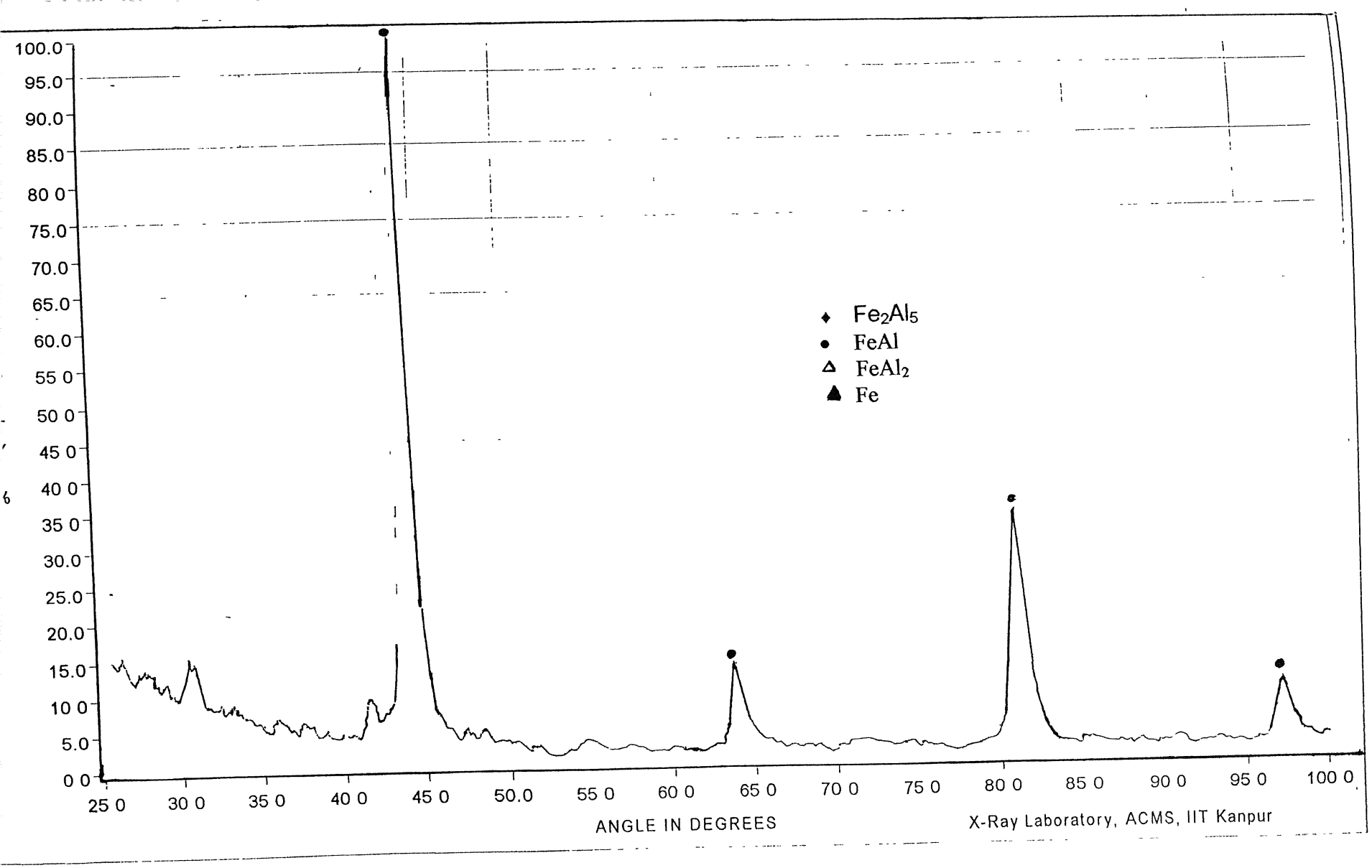

Figure 4 9 : X-Ray diffraction results of iron-iron aluminide sample Hot pressed at 900^{0}C and containing 50%Fe by weight

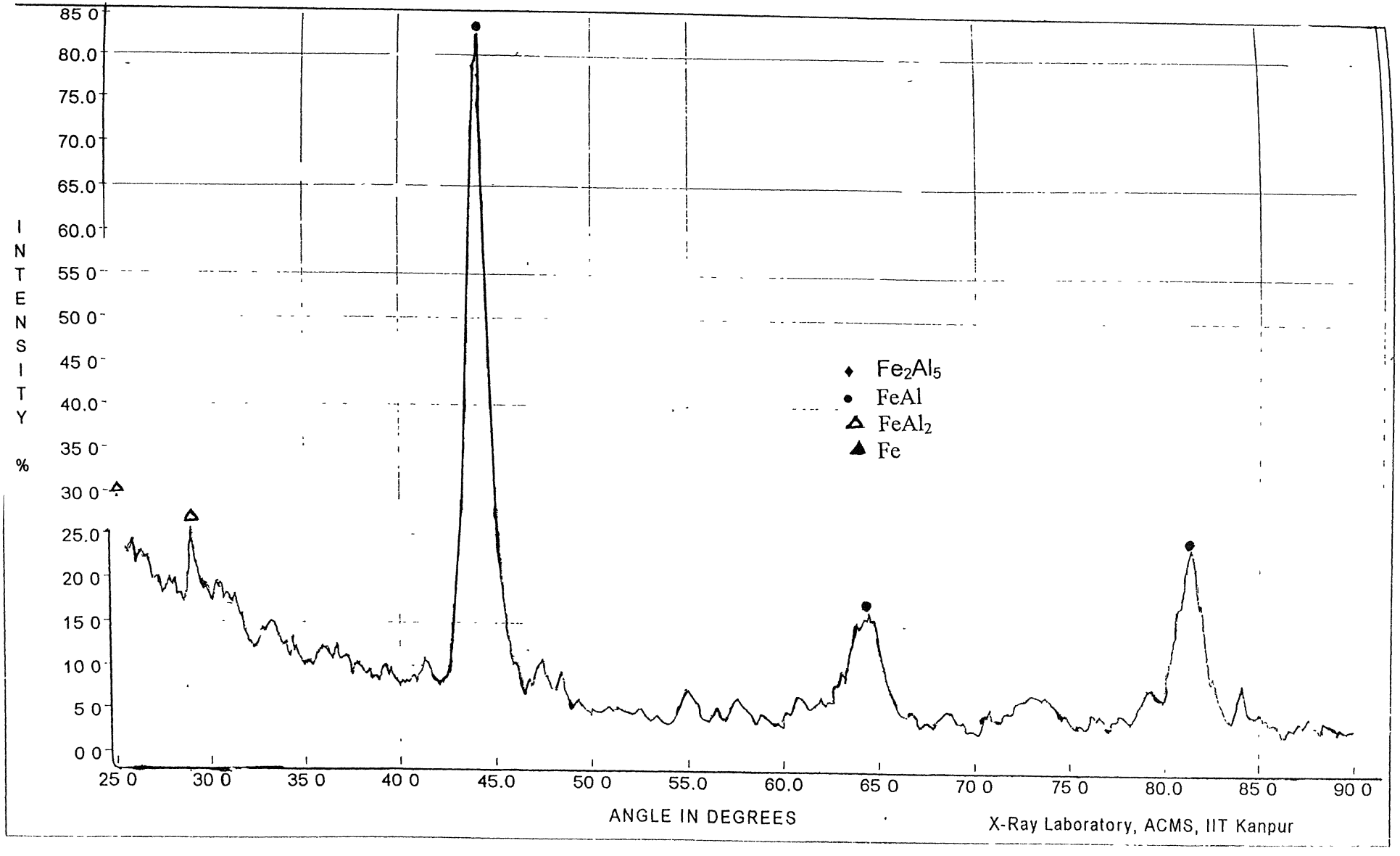

Figure 4.10 : X-Ray diffraction results of iron-iron aluminide sample Hot pressed at 950^{0}C and containing 20%Fe by weight

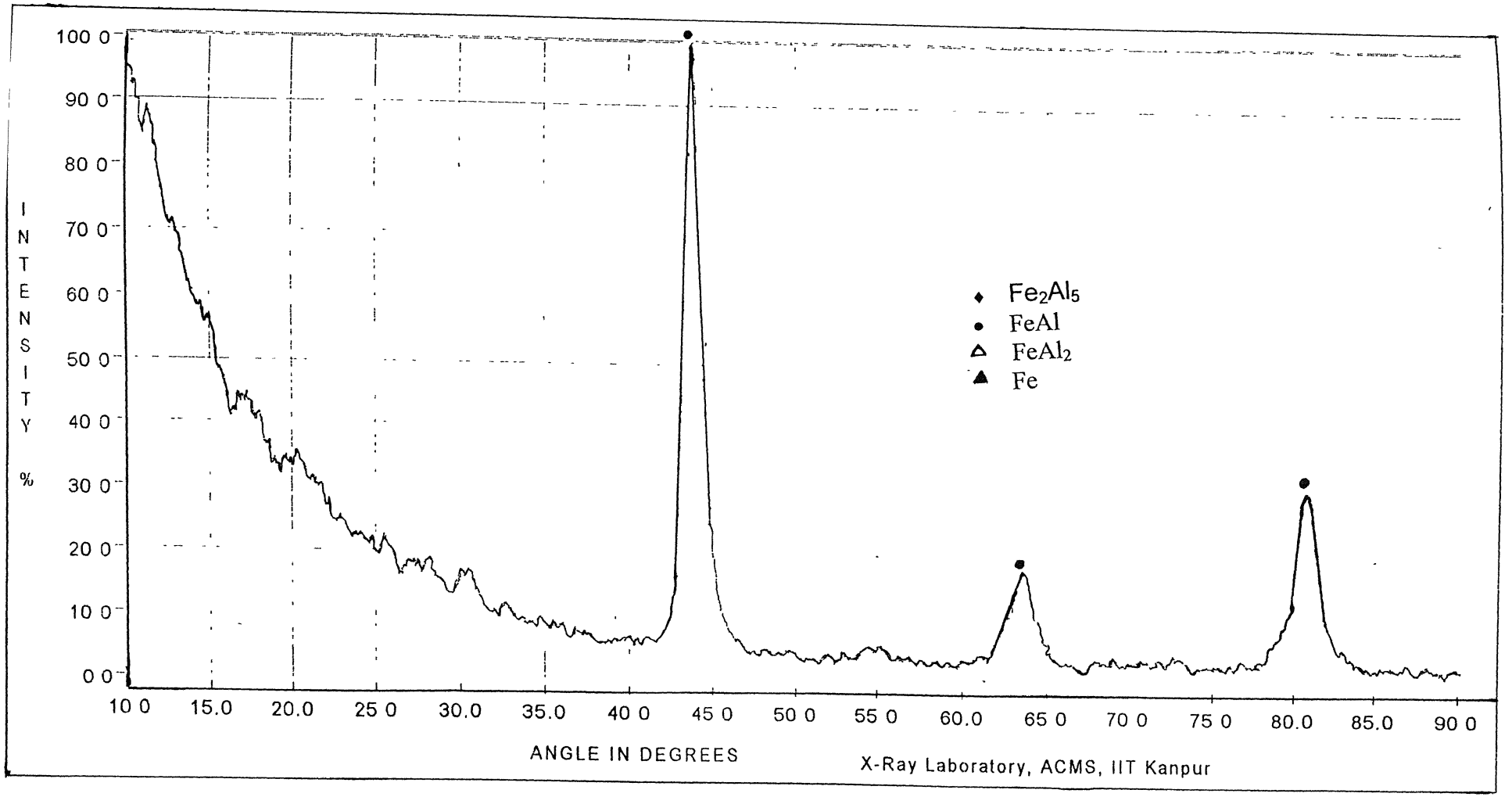

Figure 4.11 : X-Ray diffraction results of iron-iron aluminide sample Hot pressed at 950^{0}C and containing 40%Fe by weight

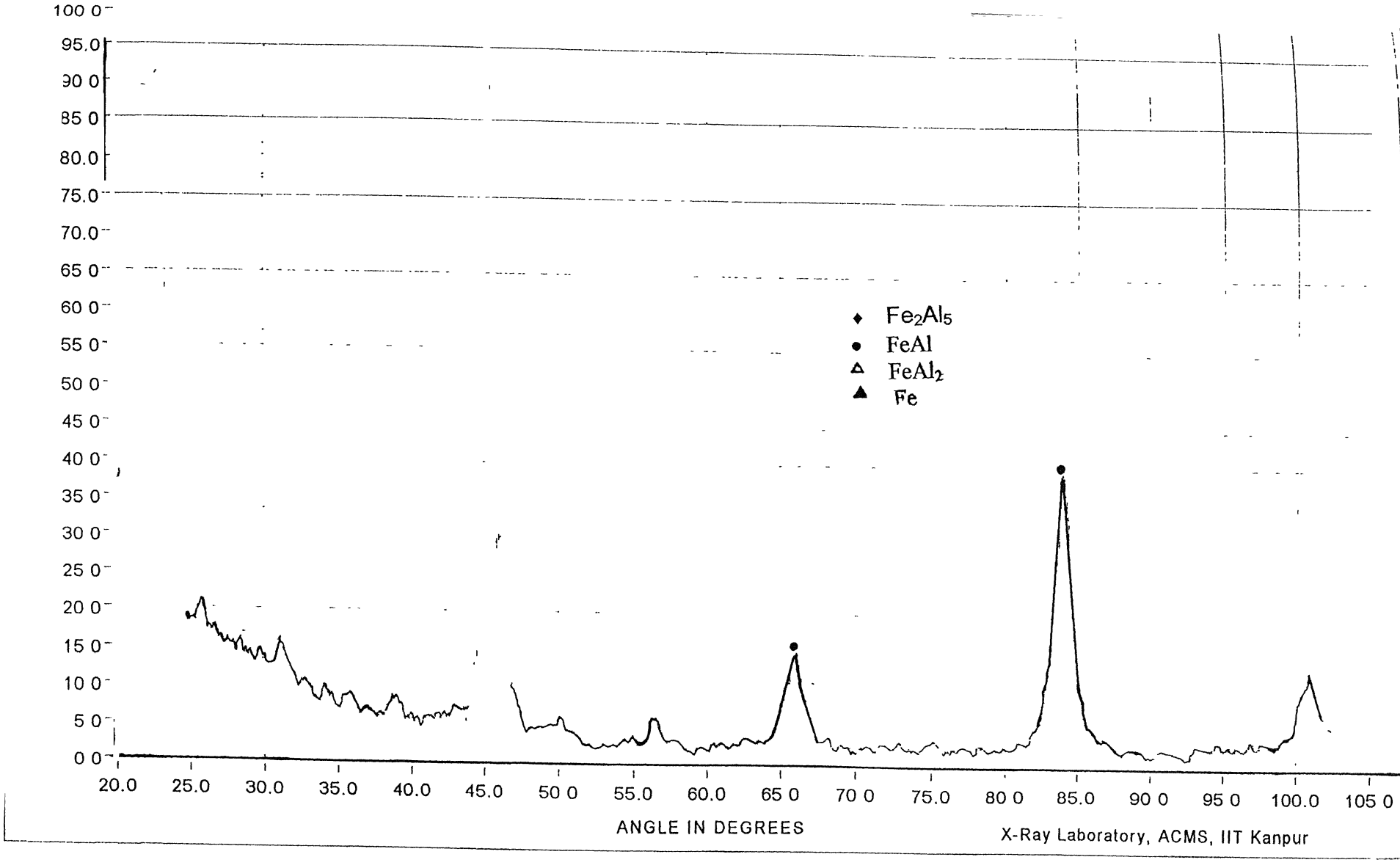

Figure 4.12 : X-Ray diffraction results of iron-iron aluminide sample Hot pressed at 950^{0}C and containing 50%Fe by weight

intermetallic phases are shown in Apendix 1. Peaks were marked with the corresponding phases. The data for all the phases is shown in Table 4.2.

The following conclusions can be drawn from the X-ray diffraction plots and Table 4.2:

(a) A single phase FeAl structure forms in the case of hot pressing of iron aluminide – iron mixture containing 50 wt% and 40 wt% respectively.

(b) Two-phase $FeAl_2$-FeAl structure form in the case of hot pressing of iron aluminide – iron mixture containing 30 wt% and 20 wt% respectively.

(c) In the case of hot pressing of iron aluminide – iron powder mixture containing 50 wt % Fe at the temperature of 800^0C, some unreacted iron is still maintained. The presence of unreacted iron was also confirmed from microhardness testing as some of the grains were found to have the hardness value of 181 VHN.

(d) In the case of powder mixtures containing 20 wt % and 30% wt % iron respectively, the intensities of $FeAl_2$ peaks are not as high as FeAl peaks indicating that volume fraction of $FeAl_2$ is low.

Table 4.2 : X-Ray Diffraction Results of Hot Pressed Samples

Wt% Fe	Hot pressing temperature(^{0}C)			
	800^{0}C	850^{0}C	900^{0}C	950^{0}C
20	FeAl+$FeAl_2$	FeAl+$FeAl_2$	FeAl+$FeAl_2$	FeAl+$FeAl_2$
30	FeAl+$FeAl_2$	FeAl+$FeAl_2$	FeAl+$FeAl_2$	FeAl+$FeAl_2$
40	FeAl	FeAl	FeAl	FeAl
50	FeAl+Fe	FeAl	FeAl	FeAl

4.3 MICROSTRUCTURAL EVOLUTION DURING HOT PRESSING OF IRON ALUMINIDE – IRON POWDER MIXTURES

As indicated by the density measurements, relative densities of hot pressed compacts varied from 0.843 to 0.99. Microstructural examination of individual hot pressed iron aluminide compacts showed that a non-uniform densification occurred in them at the hot pressing temperatures of 800°C and 850°C. At these hot pressing temperatures, thin cusped regions of nearly full densities were found to be present in the top region of the hot pressed compacts (Fig 4.13 – 4.15). Regions of incomplete densification were found to be present below these fully dense regions. In contrast, the microstructures of samples prepared by hot pressing at 900°C and 950°C were not found to have the cusped region and appeared to be almost fully densified throughout the compacts.

It is expected that the densification during hot pressing of iron-iron aluminide powder mixtures depend on

1) Iron content of the powder mixture.
2) Temperature of pressing.
3) Pressure applied and the homogeneity of its transition through the powder aggregate.
4) The holding time.

The present work aimed at keeping only the first two parameters as variables. Due to the limitations of the graphite die used for the hot pressing of the iron alumninde – iron powder mixtures, application of a

maximum pressing pressure of ~ 25 MPa only could be applied. The pressure of ~ 25 MPa was therefore kept for all the runs. Similarly, a holding time ranging between 15 –20 minutes after the desired hot pressing temperature was attained was kept for all the runs. Keeping longer holding times was not possible in the present set-up. The experimental results of the present investigation show that sufficient homogenization of the chemical composition could take place during the powder consolidation under these hot pressing conditions.

Since the hot pressing, as pursued under the present investigation, is an uniaxial single punch hot pressing operation, the load transmission through the compact was not uniform and compacts at lower hot pressing temperatures were not homogeneously densified. However, as (a) the iron percentage in the iron aluminide – iron powder mixtures increased from 20 wt % to 50 wt % and (b) as the temperature of hot pressing increased from 800°C to 850°C, the proportion of fully dense cusp regions increased (Fig 4.13 – 4.15). Such a trend in microstructural evolution of hot pressed compacts can be easily understood. As shown by Fig 4.2 [Section 4.1.2], the increasing rate of densification with increasing the iron content of the powder mixture was attributed to the role of softer iron powder in enhancing the consolidation during hot pressing. The load transmission during hot pressing became therefore better in powder mixtures containing higher iron. Similarly, by increasing the hot pressing temperature the powder mixture became softer and lead to conditions of more efficient load

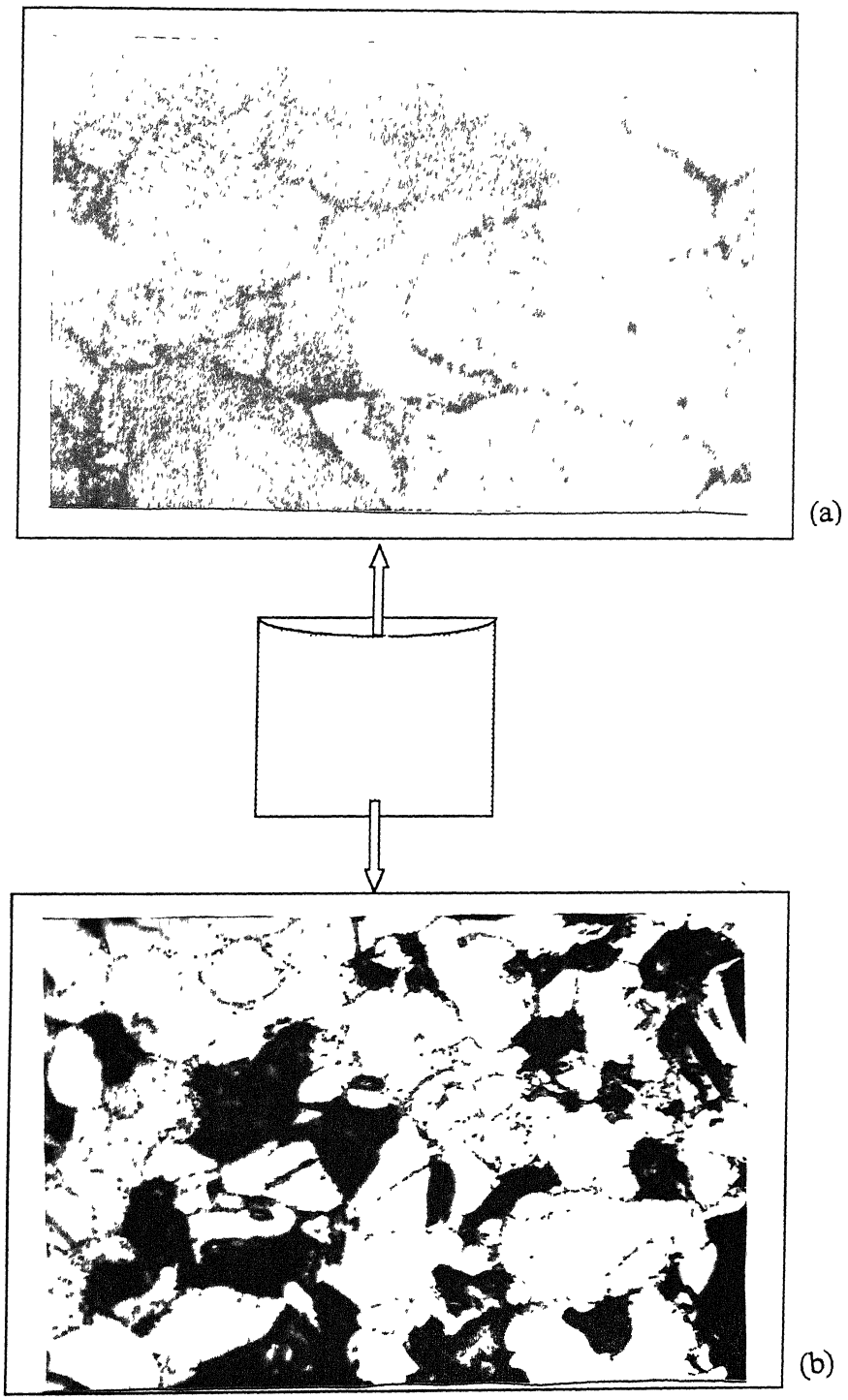

Figure 4.13 : Optical micrographs of 20%Fe sample Hot pressed at 800^0C a) top portion (500 X) b) bottom portion (200 X)

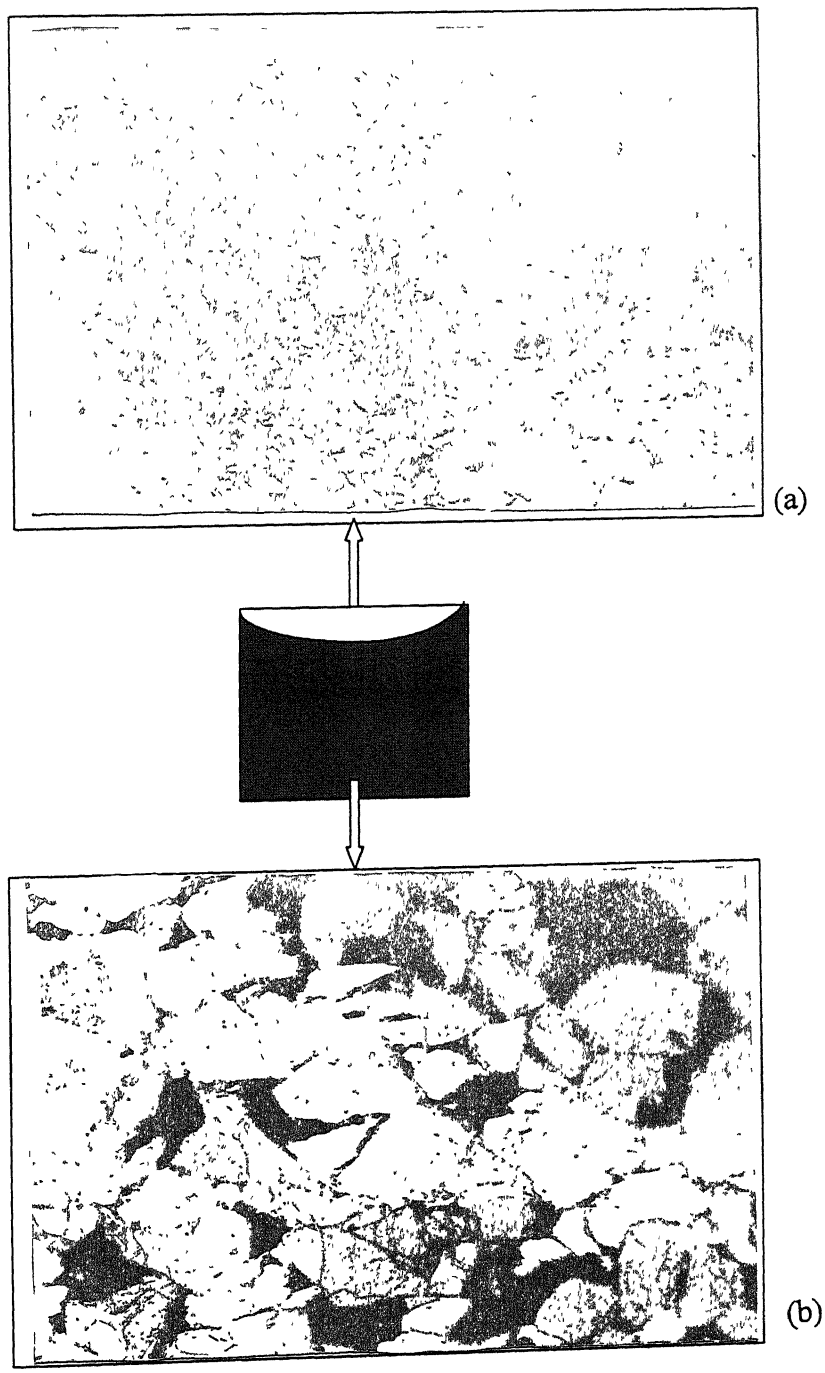

Figure 4.14 : Optical micrographs of 30%Fe sample Hot pressed at 800^0C a) top portion (200 X) b) bottom portion (200 X)

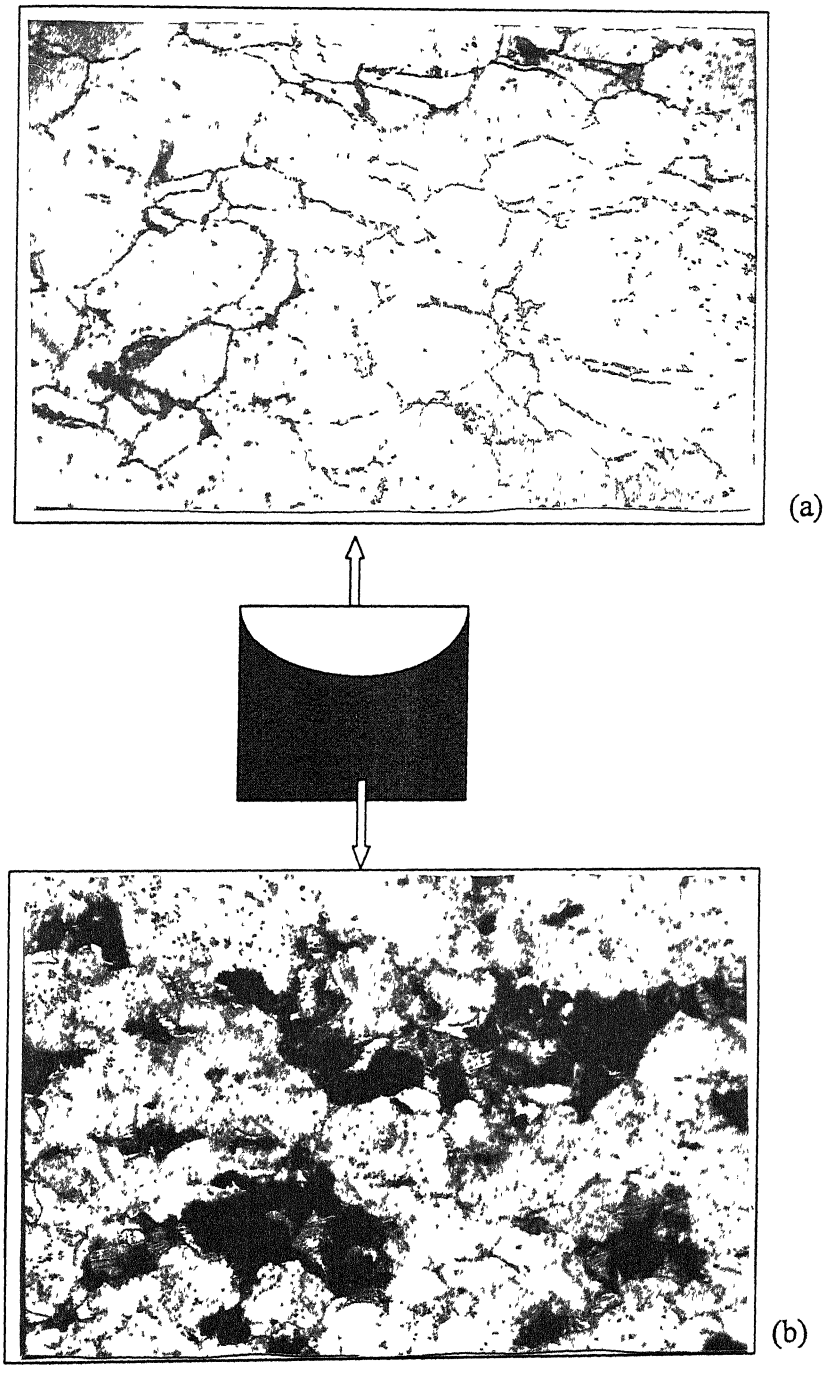

Figure 4.15 : Optical micrographs of 40%Fe sample Hot pressed at 800^0C a) top portion (200 X) b) bottom portion (200 X)

transmission through the powder mixture. Thus in both the cases the extent of fully densified cusp region increased.

Another feature that was observed in the microstuctures of (a) fully densified and (b) partially densified regions of the hot pressed compacts was that while particles/grains in fully densified regions were found to possess well rounded shape [Fig 4.13 (a)], those in partially dense regions, specially those obtained in powder mixtures containing 20 and 30 wt % Fe respectively, possessed sharp corners and edges [Fig 4.13(b), Fig 4.14 (b)]. It was also noted that as the wt % Fe increased in the powder mixtures and the iron aluminide compositions entered the single-phase FeAl region of the Fe-Al phase diagram, the flatness of particles/ grains decreased in the partially densified regions [Fig 4.15(b)]

Fig 4.16 shows microstructures of the three regions of the hot pressed compact containing 40 wt % Fe in the powder mixture and pressed at the temperature of 850°C. Different stages of powder-mixture densification, associated with full densification at the top, somewhat lower densification in the middle and much lower densification at the bottom, can be seen to be occurring in the sample. Similar observations were made in mixtures containing 20, 30, and 50 wt % Fe, but only one of these cases has been shown in Fig - 4.16. Here transition from full dense region to slightly less region was found to be very smooth. It was also observed that as temperature of hot pressing increased from 800 to 850°C the proportion of fully densified region increased.

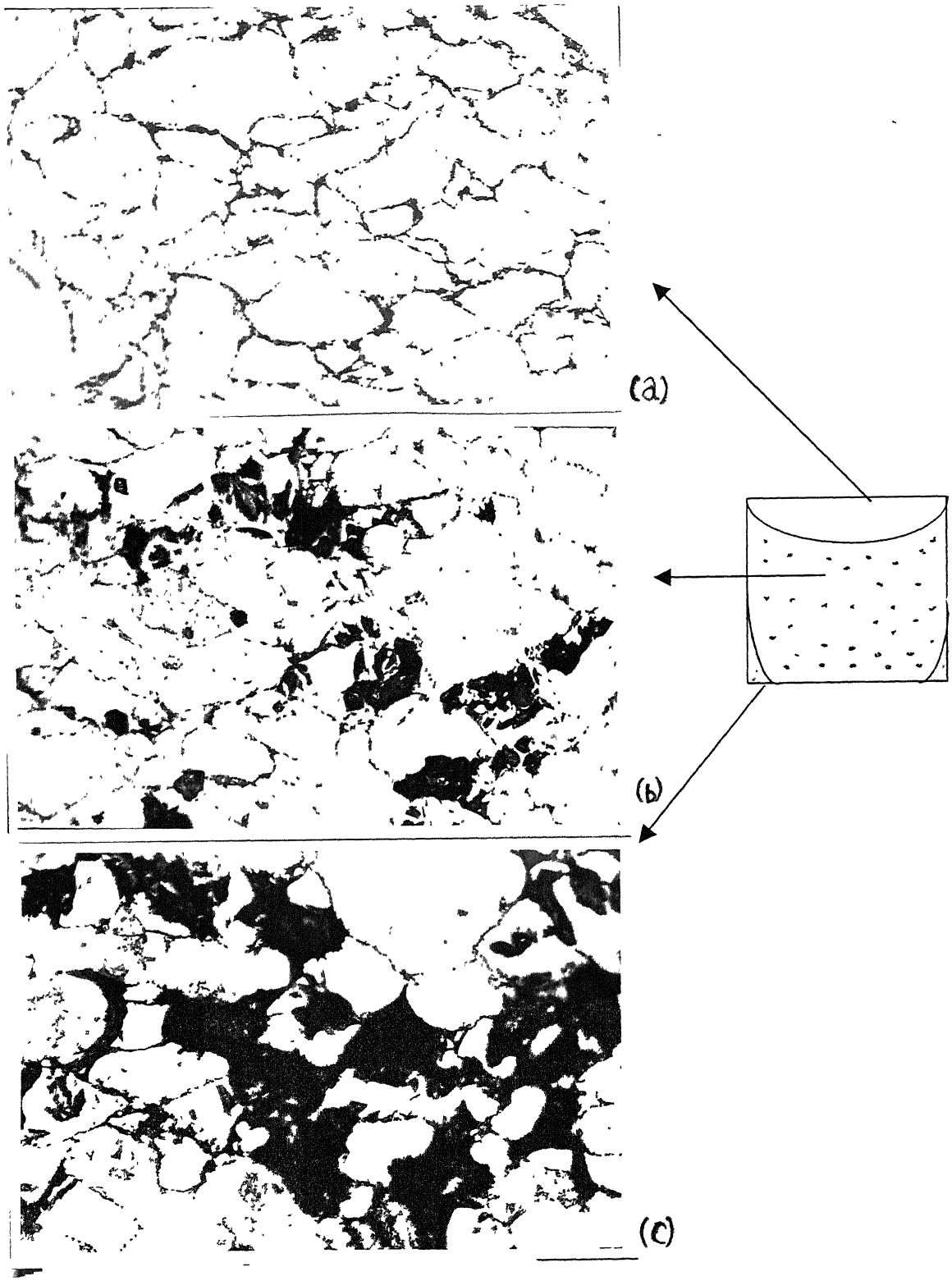

Figure 4.16 Optical micrograph of 40% Fe sample hot pressed at 850^{0}C
a) top, b)middle, c)bottom-corner (all in 200 X)

When hot pressing was done at 900 and 950^{0}C the full densification was achieved through out the region of the compact It has already been mentioned earlier that mixtures containing 20 and 30 wt % iron fall in the $FeAl_2$-FeAl region. The presence of two-phase structure was observed in their microstructures after etching and has been shown in Fig 4.17 to 4.18. Here lamellar region indicates the presence of $FeAl_2$ phase in the microstructure, and has earlier been confirmed by EPMA analysis. In contrast, as the iron percentage in the iron alumnide – iron mixtures increases from 20 to 30 wt % Fe, the volume fraction of $FeAl_2$ becomes lesser which has been observed from figure 4.17(a) and 4.18 (a). SEM microgrph of the two-phase lamellar region is shown in figure 4.19 which was observed in samples hot pressed at 900^{0}C containing 30 wt % Fe in the starting powder mixture. However, these lamellar regions totally disappeared for samples containing 50 wt % Fe in the starting powder mixtures, shown in figure 4.20. In XRD plots also no characteristic peak of $FeAl_2$ was found for hot pressed samples containing 40 and 50 wt % Fe in the starting powder mixtures.

4.4 DENSIFICATION MECHANISM:

The compact that was made is cylindrical in shape. Let the diameter and height of it is D and H respectively. The empirical relationship that exist between P_x (pressure at a distance x from the top) and X (distance from the top) is given below[23],

$$P_x = P \exp (- 4 U Z X / D)$$

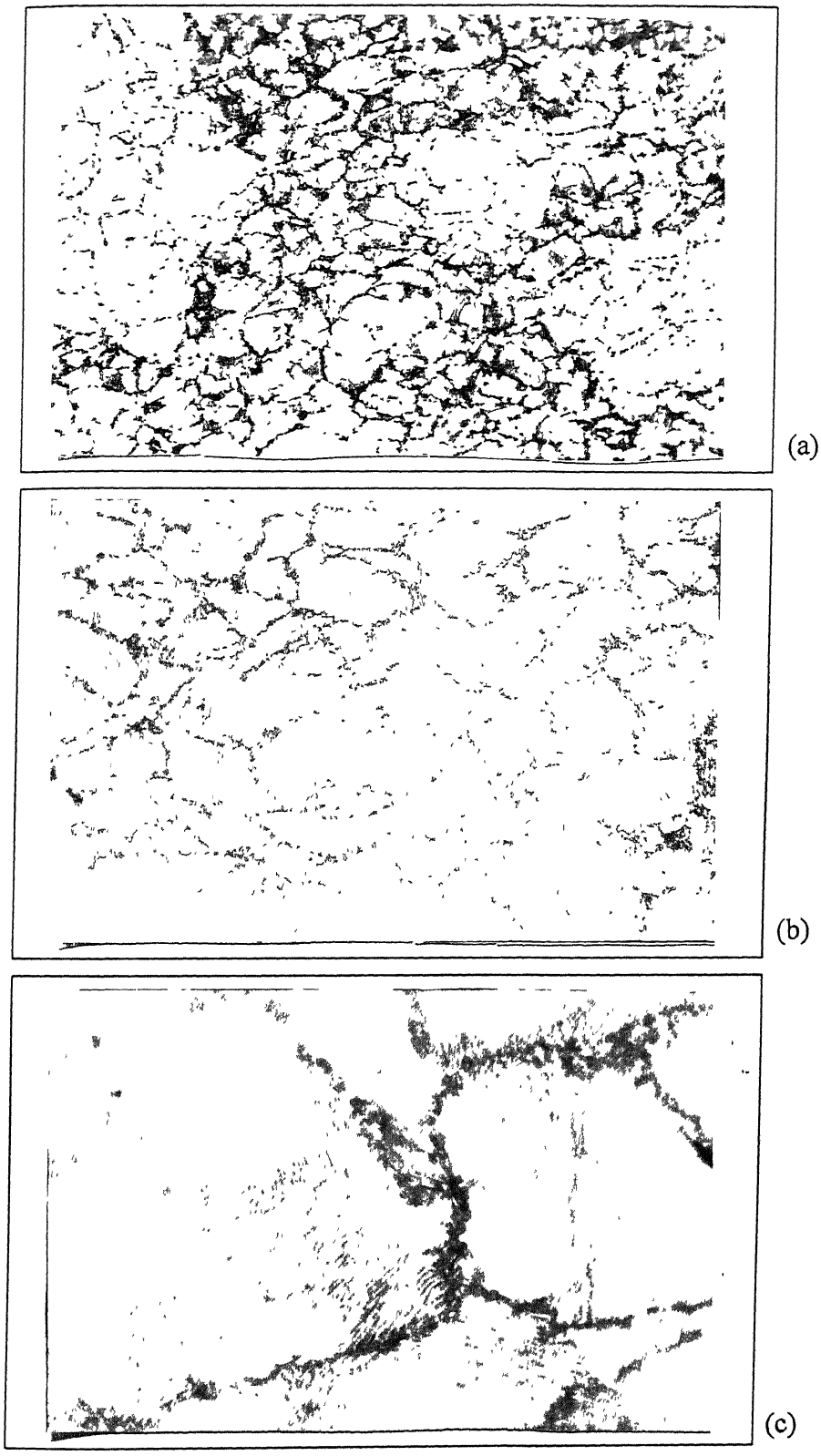

Figure 4.17 . Optical micrographs of 20%Fe sample Hot pressed at 900^0C a) 100 X, b) 200 X, c) 1000 X

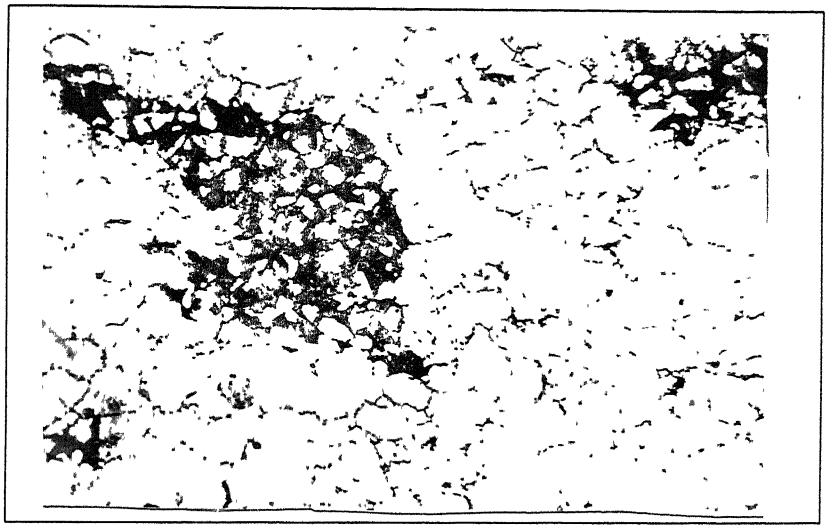

(a)

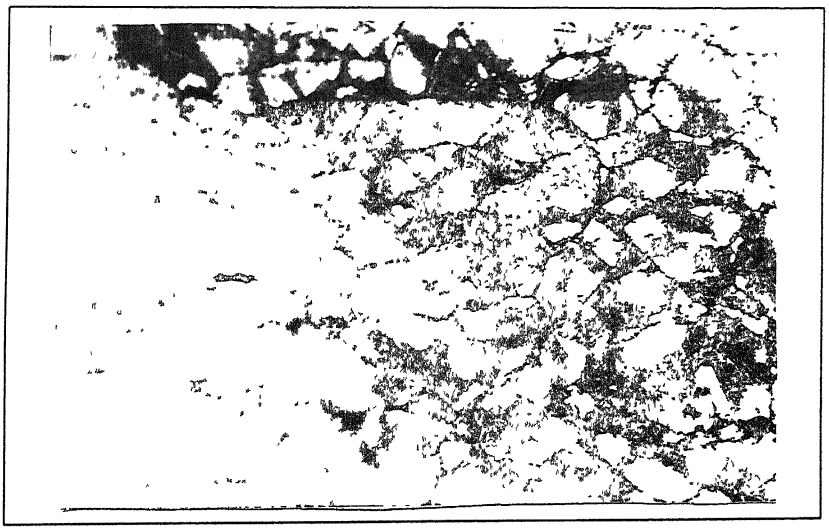

(b)

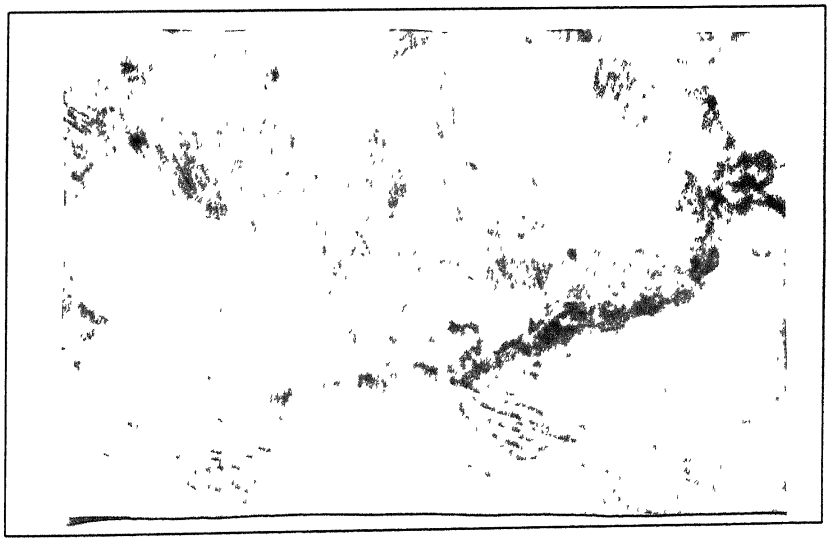

(c)

Figure 4.18 : Optical micrographs of 30%Fe sample Hot pressed at 900^{0}C a) 100 X, b) 200 X, c) 1000 X

Figure4 19Scanning electron micrograph of 900°C-30% in lamellar region

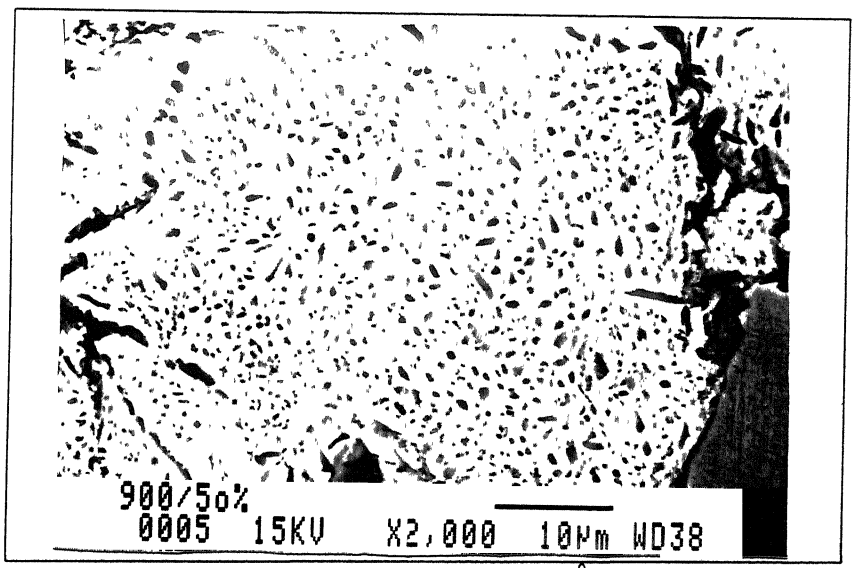

Figure 4.20Scanning electron micrograph of 900°C-50% showing no lamellar region

where P is the applied pressure, U is the coefficient of friction between powder and die wall, A is the area of cross-section, and Z is the proportionality constant. This indicates that pressure drops exponentially as the distance increases from the top surface. This is the reason why the top portion of the compact getting more densification compared to the bottom portion. In the middle the rearrangement of the particle is more compared to the surface, where friction comes into consideration. Effect of these two leads to the formation of truncated circle shaped fully dense region at the top of the sample.

During the course of hot pressing, temperature and pressure are applied simultaneously, so compaction as well as sintering takes place at the same time. As the pressure is applied particles starts to rearrange and leads to better packing. As a result of this porosity decreases and total contact area between the particles increases. The points of contacts undergo elastic deformation, and in all points residual energy is stored which results in strain hardening of the powder particles. As a result of strain hardening strength of the material increases, and elastic deformation stops at the moment it cross the effective applied stress. This does not occur in case of hot pressing, as the higher temperature does not allow the material to get strain harden. The thing that was discussed are valid for the powder particles with same composition but if mixture of two different powder is used as a starting material the two new thing comes into consideration.

1) Relative hardness of the two materials.

2) The proportion in which they are mixed.

In the present work Fe_2Al_5 is hard and brittle phase and Fe is soft phase. Two situations can appear in this case. If iron powder particle is present within the aluminide particles then it will start to flow plastically under applied pressure and temperature between the aluminide particles and fill the pores present between them. On the other hand if two aluminide particles come in contact and pressed each other then cracks start to appear on the aluminide particle. This has been observed When hot pressing was done at low temperature (800^0C) and for 30%Fe, shown in figure 4.14(b). These cracks lead to the fracture of the particle. These fractured particles concurrently rearrange themselves under the applied load resulting into better packing. In hot pressing as densification progresses, grain boundary and volume diffusion process become controlling factor. Temperature is critical factor for diffusion. Diffusional creep mechanism is the dominating process in hot pressing where climbing of dislocation is rate controlling step. As binary mixture of powder was used so homogenization during hot pressing is also to be kept in to consideration. The compositional gradient associated with mixed powder enhances the diffusional fluxes, which contribute to sintering. The diffusion rates determine the rate of homogenization during hot pressing. Initially concentration gradients are steep. With prolonged heating, the gradient

level out. Generally small particle size, higher hot pressing temperature and longer Hot pressing times promote homogenization.

It is worth mentioning that hot pressing of iron-iron aluminide powder mixture not only causes densification of the powder, it also helps in phase modification, as revealed by X-ray diffraction results and consequent evolution of their morphology. These other aspects of microstructural changes involving formation of new phase(s) and their morphological distribution in the structure was indeed found to be occurring in samples prepared by hot pressing route. So in brief the densification mechanism is lying on the (i) fracturing and fragmentation of aluminide particles, (ii) plastic flow of iron particle to fill up the neighboring pores, (iii) diffusion of Al and Fe across the particle boundary.

4.5 COMPRESSIVE STRENGTH OF HOT PRESSED COMPACT

Room temperature compression was done on the samples prepared at the hot pressing temperature of 850^0C 900^0C and 950^0C with mixing 30 40 and 50 wt% iron to the starting material. Compression testing was done on MTS testing machine as well as on RIEHELE compression testing machine. Typical load-displacement curves obtained during compression testing on MTS machine are shown in Appendix-2. The compressive strengths of different hot pressed samples are shown in Table 4.3 and are shown in Fig 4.21. It was observed that the compressive strength of hot pressed samples increased with increasing the hot pressing temperature for the same amount of addition of iron in the

Table 4 3: Compressive strength (**Mpa**) of the hot pressed samples

Wt% Fe	Hot pressing temperature (^{0}C)			
	800^{0}C	850^{0}C	900^{0}C	950^{0}C
30		307.40	894.91	955.30
40	224.59	491.92	1046.44	1374.05
50		660.07	1310.16	1428.70

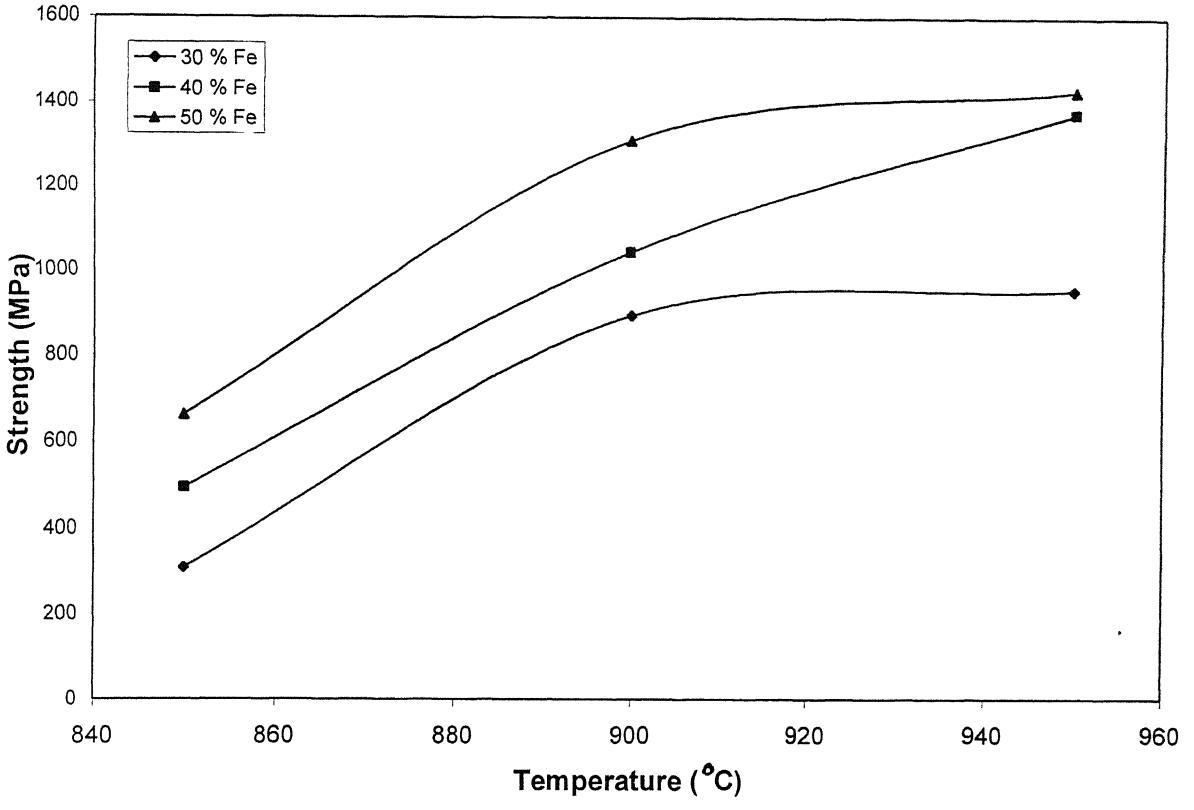

Figure 4.21 **Plot showing variation in strength with increase of hotpressing temperature for different Fe %**

powder mixtures. It was also observed that by keeping the hot pressing temperature same the strength value of the processed material increases by increasing the proportion of Fe in the starting powder mixture (Fig 4.22).

In principle the strength value of the compact depends on the parameters such as a) grain boundary strength, b) presence of second phase, c) amount of thermal vacancies, d) antisites, e)grain size, f)presence of Al_2O_3 coming from powder route. Directly from the literature it can be mentioned that the concentration of thermal vacancy type defects increases with increasing Al concentration in the 45-50 at.% Al range[33]. However, it is also mentioned that the constitutional disorder in Fe - (40 to 45 at.%) Al is due to antisite atom pairs rather than vacancies. These factors come into the consideration if post heat treatment (prolonged annealing) is done of the hot pressed compacts. On the other hand, If the grain size is decreased after deformation through heat treatment then also strength value increases [22]. But in present wok as concentration was given on only deformed product. So the grain boundary strength, the porosity content and presence of second phase plays the vital role in determining the strength value. It is mentioned in the literature that at the Al rich phases the fracture mode is intergranular while it is transgranular type for Fe rich side of the phase diagram [20]. The presence of a higher iron content in the starting iron-iron aluminide powder mixture improves its compressibility. Therefore the volume fraction of pores in compact

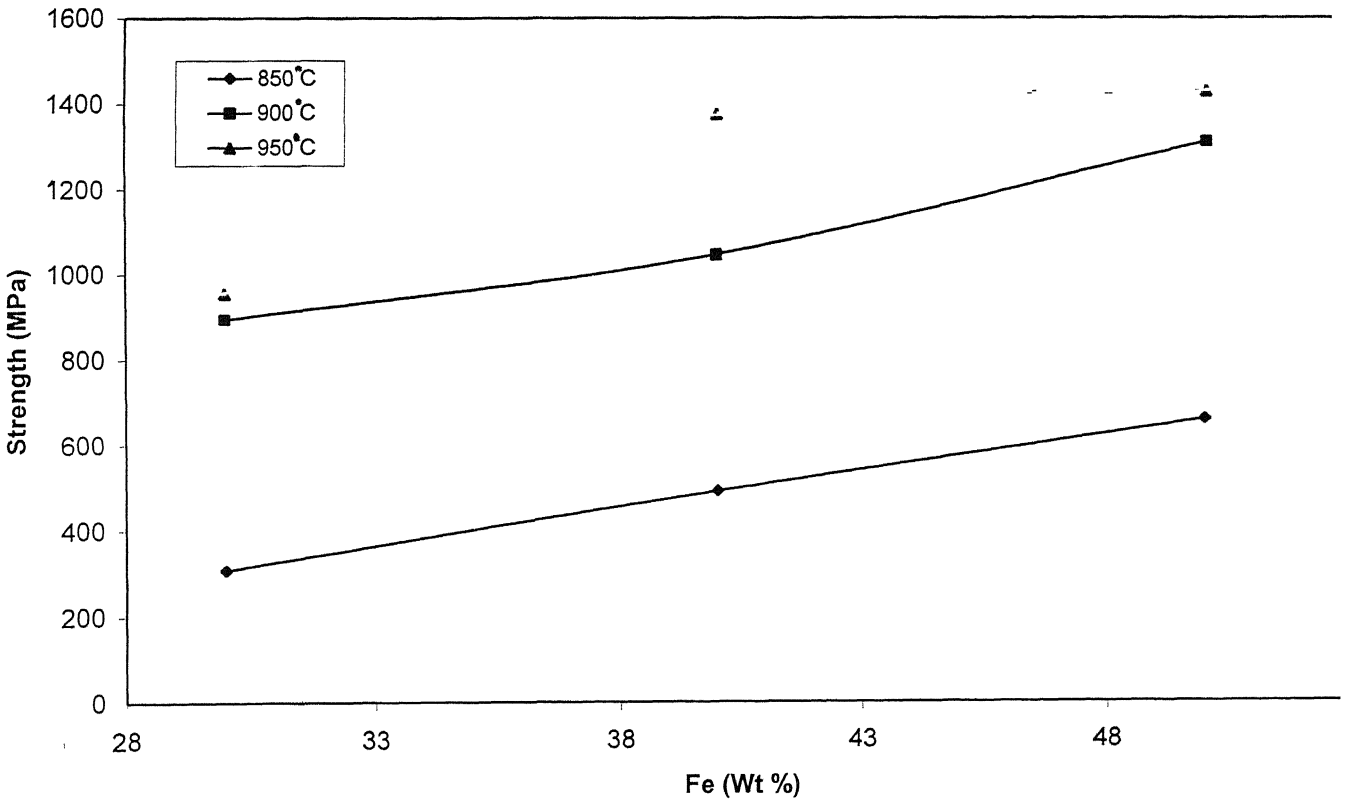

Figure 4.22 **Plot showing variation in strength with increase in Fe % for different hot pressing temperature.**

containing higher Fe content is lower. Further, since the reduction of porosity in iron-iron aluminide powder compacts in the early stage of hot pressing is achieved by the plastic flow of iron particles, the contiguity between aluminides and iron powder particles improves in powder mixture containing higher iron content. On the other hand with increase in hot pressing temperature results in better diffusion through interparticular region and improves the strength at the boundary. So the shape of the curves as shown if figure 4.21 and 4.22 showing compressive strength of the compacts at different processing condition can be understood in above manner.

CHAPTER FIVE

CONCLUSIONS

1) Single/multiple phase iron aluminide can be prepared by P/M processing of mixture of iron and iron aluminide powder containing Fe_2Al_5 – $FeAl_2$ phase mixture.

2) $FeAl_2$-FeAl two-phase iron aluminide compacts can be obtained by the hot pressing of iron aluminide – iron powder mixture containing 20 wt.% and 30 wt.% Fe by hot pressing at 800^0C to 950^0C

3) FeAl single phase compacts can be obtained by hot pressing of iron aluminide – iron powder mixtures containing 40 wt.% and 50 wt.% Fe by hot pressing from 800^0C to 950^0C. However, samples obtained from powder mixtures containing 50 wt % Fe may require longer homogenization time after hot pressing as some unreacted iron was found to remain in them.

4) Fully dense iron aluminide compacts can be obtained by hot pressing the iron aluminide – iron powder mixtures at the compaction pressure of ~ 25 MPa if hot pressing is done at 900 to 950^0C irrespective of the composition of the powder mixture.

5) Complete elimination of pores in iron aluminide – iron powder mixtures, containing 20, 30, 40 and 50 wt % Fe, is not achieved if the hot pressing is carried out at the pressure of ~ 25 MPa and at temperatures of 800^0C and 850^0C However, under these hot

pressing conditions, pore elimination is enhanced with the increase in Fe% in the starting powder mixtures.

6) Higher iron percentage in the initial powder mixture leads to better densification and better strength in the particle boundary and more rounding of the particles/grains. As a result of this the strength of hot pressed iron aluminide compacts increases with increasing the iron percentage in the starting iron aluminide – iron powder mixtures.

7) If hot pressing temperature increases then also strength value increases. Which is due to better diffusion, more plastic flow the softer phase(Fe) in between hard particle. This is the is the reason for getting better strength value at higher hot pressing temperature.

CHAPTER SIX

SUGGESTION FOR FUTURE WORK

Only Uniaxial Hot Pressing was followed as a hot consolidation technique in the present work but there are other consolidation techniques also present like hot forging, hot extrusion, and hot isostatic pressing. So following suggestion can be given in this regard.

1) Observation of the consolidation in other in other hot consolidation technique.
2) Few alloying addition (Zr, Mo, B)suggested in literature can be made in the initial powder mixture for the improvement in properties of the product.
3) Further heat treatment like annealing and then slow cooling or quenching can be done on the samples to note their change in properties.
4) Density distribution or density mapping can be done by measuring void fraction through computer added digital scanning of the specimen cut along the radial-axial plane.
5) In the above method volume fraction of second phase can also be calculated.
6) In present work the processing parameters considered are temperature of hot pressing and the proportion of softer phase. So further experiment can be done to determine the effect of pressure and dwell time also.

APENDIX-1

2θ Values for 5 High Intensity Peaks of Iron Aluminide

Phase	Intensity	2θ		h	k	l
		CuKα λ=1.54056 A	CrKα λ=2.20897 A			
FeAl	100	44.186	67.975	1	0	0
	25	81.503	151.194	2	1	1
	14	64.316	46.521	2	0	0
	8	97.593	104.287	2	2	0
	8	30.818	86.556	1	0	0
Fe_3Al	100	44.186	67.975	2	2	0
	19	81.286	150.967	4	2	2
	12	64.256	104.450	4	0	0
	8	114.474	—	6	2	0
	7	26.627	40.029	1	1	1
$FeAl_2$	100	18.988	28.381	$\underline{1}$	1	1
	80	20.994	31.421	0	4	0
	80	24.836	37.279	$\underline{2}$	1	1
	80	25.201	37.838	$\underline{1}$	4	0
	80	26.790	40.280	0	3	1
Fe_2Al_5	100	42.823	65.719	0	0	2
	100	44.141	67.899	1	3	0
	40	27.857	41.926	0	2	0
	25	23.022	34.974	2	0	0
	16	62.726	101.347	2	4	0
$FeAl_3$	100	44.832	69.049			
	83	43.472	66.790			
	20	64.177	104.287			
	17	21.819	32.674			
	11	24.164	36.281			
Fe_4Al_{13}	100	43.253	66.429	$\underline{3}$	2	5
	100	44.369	68.275	$\underline{2}$	3	4
	100	44.832	69.049	$\underline{4}$	0	6
	60	24.164	36.251	$\underline{3}$	0	3
	60	25.135	37.738	2	2	0

APENDIX-2

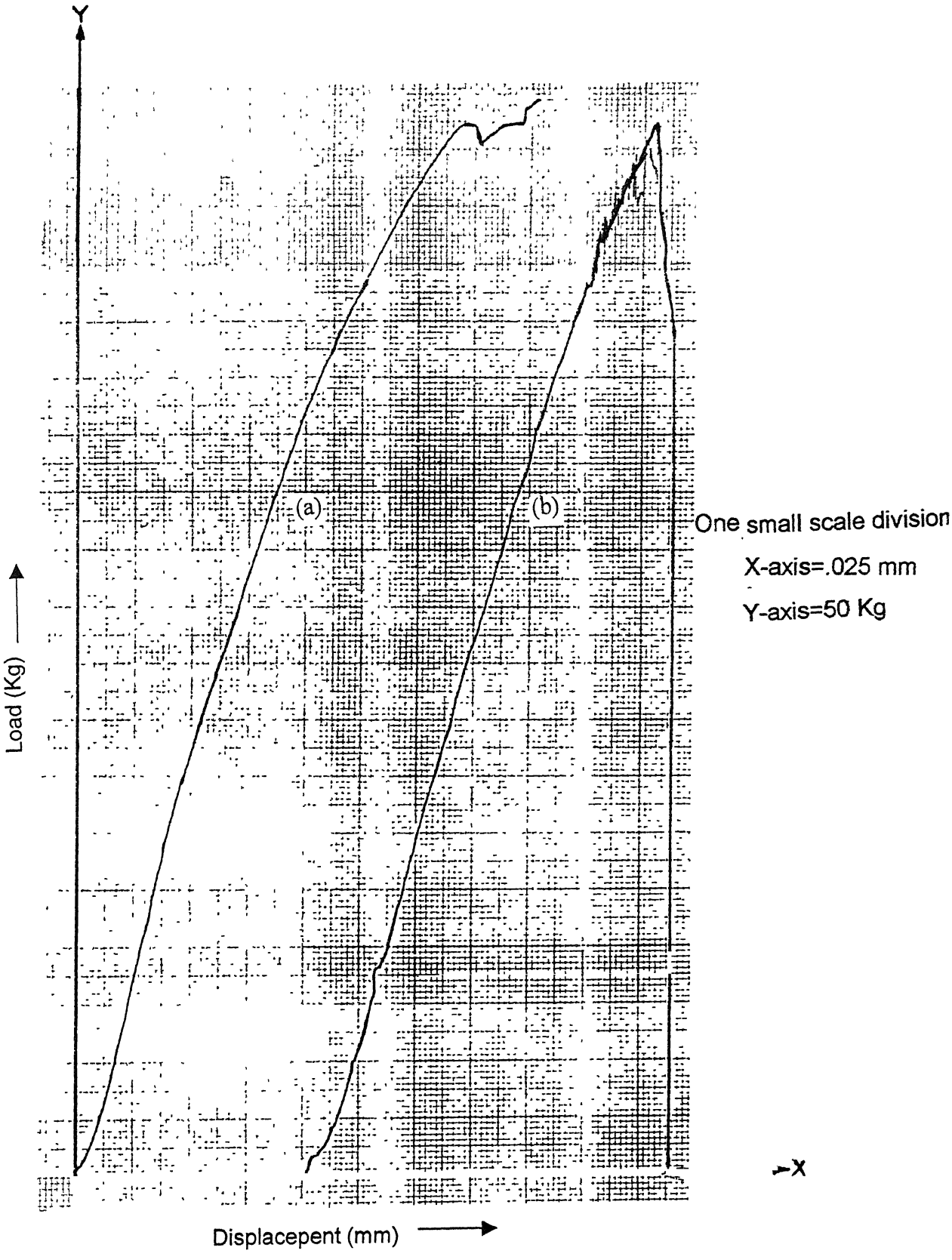

Typical load vs. displacement curve for hot pressed samples a) 900^0C-40% b) 900^0C-30% (each have cross section area .882cm^2 and cross head speed is .5mm/min)

REFERENCES

1. N. S. Stoloff; "Ordered Alloys – Physical Metallurgy and Structural Applications" ; Int. Met Review ; 29 (1984); pp123-135.

2. Gerhard Sauthoff ; " Intermetallic Phases – Material Developments and Properties" ; Z Metallkde.; 80(1984); pp-337-344.

3 C T.Liu, J.O.Stiegler, "Ordered Intermetallic", Properties and Selection: Non-ferrous Alloys and Special Purpose Materials; Metal's Handbook; vol 3; 10th ed; ASM International, 1990; p-913

4 C T.Liu, K S Kumar; "Ordered Intermetallic Alloys,Part I, Nickel & Iron Aluminides" ; JOM, 1993 , p-38.

5 C T Liu, K.S.Kumar ; "Ordered Intermetallic Alloys , Part II , Silicides, Trialuminides and Others"; JOM ; June 1993 ; p-28.

6 C G McKamey, J A.Herton, C T.Liu; "High Temperature Ordered Intermetallic Alloys II" , ed. by N S Stoloff, C.C.Koch, O.I.Zumi, C.T Liu; MRS Symp Proc. ; vol.81; MRS; Pittsbergh;1987 ,p-32.

7 C.C.Koch, C.T.Liu, N S.Stoloff; eds., High Temperature Ordered Intermetallic Alloys (Pittsbergh, PA MRS,1985).

8. N.S.Stoloff et al; eds., High Temperature Ordered Intermetallic Alloys II (Pitsbergh,PA.MRS,1987)

9. C T.Liu et al; eds., High Temperature Ordered Intermetallic Alloys II; (Pitsbergh,PA:MRS,1987).

10. Hugh Baker; "Alloy Phase Diagram", ASM Handbook ; vol. 3 , 1992; p-2.44.

11 R.A Buckley, H.jones, C.M Sellers; "Structure and Properties of Ordered Intermetallics Based On The Fe-Al System", ISIJ International; vol.31; 1991, no.10, p-1113

12 U,Prakash, R A Buckley, H jones, C M.Sellers; "Structure and Properties of Ordered Intermetallics Based On The Fe-Al System"; ISIJ International; vol 31; 1991; no.10 ; p-1113

13 C.G.McKamey et al; J. Mater.Res.; 6(1991) ; p-177.

14 J.H.Devon; "Oxidation of High Temperature Intermetallic" , ed. T Grodstein, J.Doychak; (Warrendale, PA:TMS , 1989); p-107.

15 D.G.Morris, M.Nazmy, C Noreda; "Creep Resistance In A New Alloy Based On Fe_3Al" ; Scr. Met. et Mater. ; vol.31 ; no.2 ; 1994 ; p-173.

16 I.Jung, M.Rudy, G.Sauthoff; "High Temperature Ordered Intermetallic Alloys II; ed By N.S.Stoloff, C.C.Koch, O.I.Znmy, C.T.Liu; MRS Symp. Proc ; vol.81; MRS; Pittsbergh(1987) ; p-321.

17 Z.Zhonghur, S.Yanashan, G.Jun, "Effect of Niobium Addition On The Mechanical Properties of Fe_3Al Based Alloys" ; Scr Met. et Mater.; vol.33 , no. 12, 1995; p-2013.

18. J D.Whitenberger; "The Influence of Grainsize and Composition On Slow

Plastic Flow In FeAl Between 1100 to 1400 K"; Mat. Sc. & Engg.; vol.77 ; 1986 ; p-103.

19. N.S.Stoloff, G.E.Fuchs, A.K.Kuruvilla, S.Choe; "High Temperature Ordered Intermetallic Alloys II"; ed. by N.S.Stoloff, C.C.Kocxh, O.Izumy, C.T.Liu, MRS Symp Proc ; vol.81, MRS; Pittsbergh; 1987; p-247.

20 M.A.Crimp, K M.Vedula, D J.Gaydosh "Room temperature tensile ductility in powder processed B2 FeAl alloys.

21 M.K Jadava "M Tech Thesis " August 1999

22 P J.Maziasz, D.J.Alexander, J.L.Wright and V K.Sikka. "High strength, ductility and toughness in new P/M FeAl intermetallic alloys".

23. R.M German ;Powder Metallurgy Science, chapter 6.pp 212-216.

24 V.K Sikka "Processing and applications of iron aluminide". The mineral and materials socity 1994 .

25 Dr. Phil Max Mansan; "Constitution of Binary Alloys"; ed. by Dr. Rer Nat. kurt Anderko, McGrawhill Book Company, INC; 1958.

26. E H Hollingsworth, G.R.Frank,Jr., R E Willet, Trans. AIME; 224; 1962; pp188-189.

27 D.U.Rabin, R.N Wright; "Synthesis of Iron Aluminide From Elemental Powders, Reaction mechanism and Densification Behaviour" ;Met. Trans. A; vol 22a; Feb.1991, p-277.

28. D K.Mukhopadhyay, C.Suryanarana, F H.fores, Structure Evolution in Mechanically alloyed al-Fe Powders."

29. F.H Fores, C.Suryanarayana, P.R.Taylor, C.M Ward-Close, and P.Goodwin, "Syntesis of Advanced Light Weight Metals by Powder Metallurgy techniques"

30. H Xiao, I.Baker "The relationship between point defects and mechanical properties in Fe-Al at room temperature" Acta metall.mater.vol 43 No.1 pp 391-396 1995.

31 Animesh Bose. "Review of current and advanced hot densification process".

32. M.FSayre. "Compression tests" ASM Metal Handbook.Edition1948 pp109-111.

33. R.A.Varin, J.Bystrzycki, A.calka "Characterization of nanocrystaline Fe45 at.%Al intermetallic powders obtained by controlled ball milling and the influence of annealing". Intermetallics 7 (1999) 917-930

A-133082

Date Slip

The book is to be returned on the date last stamped.

.....	.....
.....	.....
.....	.....
.....	.....
.....	.....
.....	.....
.....	.....
.....	.....
.....	.....
.....	.....
.....	.....
.....	.....